

N66-13991

FACILITY FORM 802

(ACCESSION NUMBER)	59	(THRU)	
(PAGES)	CP 68891	(CODE)	06
(NASA CR OR TMX OR AD NUMBER)		(CATEGORY)	

Development of Cathodic Electro-
catalysts for Use in Low Temperature
H₂/O₂ Fuel Cells with an
Alkaline Electrolyte

Contract No. NASW-1233

GPO PRICE \$ _____

CFSTI PRICE(S) \$ _____

Hard copy (HC) 3.00

Microfiche (MF) .50

ff 653 July 65

Q-1

First Quarterly Report

Covering Period July 1
Through September 30, 1965

for

National Aeronautics and Space
Administration
Headquarters, Washington, D. C.

Tyco Laboratories, Inc.
Bear Hill
Waltham, Massachusetts 02154

DEVELOPMENT OF CATHODIC ELECTROCATALYSTS FOR USE
IN LOW TEMPERATURE H_2/O_2 FUEL CELLS WITH AN
ALKALINE ELECTROLYTE

Contract No. NASW-1233

Q-1
First Quarterly Report
Covering Period July 1
Through September 30, 1965

for
National Aeronautics and Space
Administration
Headquarters, Washington, D. C.

NOTE

This is the first quarterly report of an experimental program for the development of fuel cell electrocatalysts for oxygen reduction. This work is being carried out for the National Aeronautics and Space Administration under contract NASW-1233 technically monitored by Mr. E. Cohn. Principal Investigators are A. C. Makrides, R. J. Jasinski, and J. Giner.

CONTENTS

	<u>Page No.</u>
I. INTRODUCTION	1
II. EXPERIMENTAL METHODS	4
III. RESULTS	14
APPENDIX A	45
APPENDIX B	49

LIST OF FIGURES

<u>Figure</u>		<u>Page No.</u>
1	Rotating Disc Electrode	5
2	Rotating Electrode Cell	7
3	Floating Electrode Cell	12
4	i(E)-curve for Pt	19
5	i(E)-curve for Au	20
6	i(E)-curve for Ag	21
7	i(E)-curve for Ta	22
8	i(E)-curve for Zr_2Ni	23
9	i(E)-curve for TiNi	24
10	i(E)-curve for NbPt	25
11	i(E)-curve for TiCu	26
12	i(E)-curve for $TaPt_2$	27
13	i(E)-curve for $TiPt_3$	28
14	i(E)-curve for $TaNi_3$	29
15	i(E)-curve for $TaPt_3$	30
16	i(E)-curve for $TiCu_3$	31
17	i(E)-curve for $ZrAu_3$	32
18	i(E)-curve for $NbNi_3$	33
19	i(E)-curve for $TiNi_3$	34
20	i(E)-curve for $TiCr_4$	35
21	i(E)-curve for WC	36
22	i(E)-curve for Cr_3C_2	37
23	i(E)-curve for TiC	38
24	i(E)-curve for Ni_3B	39

I. INTRODUCTION

The objective of this program is to investigate, in the least ambiguous manner, a large number of electrically conductive materials over a relatively wide range of composition and structure for catalytic activity in the electro-reduction of oxygen. Materials screened in this manner are to be developed as cathodes for low temperature hydrogen-air fuel cells employing alkaline electrolyte.

Basically, two approaches are being used in selecting the materials for this study. In one approach, the structure is the criterion of selection. Specifically, intermetallic compounds, including interstitials such as borides, nitrides, silicides, carbides, and oxides will be studied. The structure classification is given in Appendix A. In the second approach, compounds will be selected according to atomic considerations or because of previous work with related systems, for example, spinels or special solid solutions. Comparison of alloys having a common element with each other and with pure elements will help to ascertain the relative importance or contribution of structure versus that of the atomic components.

Since the surface of the material in contact with the electrolyte assumes a composition corresponding to its galvanic potential, (by oxidation, leaching of surface atoms, etc.) the difference between surface and bulk composition at the working potential of an oxygen (air) cathode will have to be taken in account and, when possible, investigated.

A. Materials

A close examination of the literature and discussions with people in the field of catalysis showed that preparations of highly dispersed metal powders by precipitation, decomposition, or reduction of salts are all beset by difficulties in obtaining well-defined alloys. It is apparent that in general one does not know even with simple systems, e.g. Ni-Cu, whether material prepared by one of these methods is a homogeneous alloy, a mixture, or perhaps a unique,

low-temperature alloy form. Therefore, we have decided to postpone examination of such materials to the second quarter of the program, after we shall have built a backlog of experimental information with alloy systems whose structure could be ascertained without doubt.

Alloys are prepared from the melt in the initial phase of this program. Arc-melting, which yields well-defined, homogeneous alloys, is being used at present. The least ambiguous procedure for identifying the alloy, provided the phase diagram is known, is by metallographic examination, which shows whether a second phase is present or not. By starting with known quantities of each component and by ascertaining that a single phase is produced, we can achieve an unambiguous characterization to a degree of sensitivity higher than that of either chemical or X-ray analysis. Supplementary measurements are made whenever there is doubt about the structure of the material. All binary or ternary systems with known phase diagrams can be treated in this way. In cases where the phase diagram has not been determined, the phase or phases present must be identified.

B. Testing Procedures

A convenient method of testing a material for corrosion resistance and catalytic activity is to use the material as a solid ingot. As such it can be mounted in an alkali resistant resin and tested potentiostatically as a rotating disc electrode run consecutively in N_2 - and O_2 - saturated KOH-solution.

By potentiostatic measurement of the corrosion current under an inert atmosphere we can not only estimate the dissolution rate under open circuit conditions, but also measure the corrosion behavior over the whole potential region which is relevant to performance as an oxygen electrode. It is likely that in certain cases a material which corrodes at too high a rate on open circuit is nevertheless acceptable because it passivates in the region of positive potentials where oxygen is reduced.

The advantages of this method are that the samples can be prepared with relative ease and speed, and have well-defined surfaces. These can then be tested unequivocally for corrosion and reasonably well for O_2 -activity under well-defined transport conditions (Levich equation). The disadvantages of the method are: (a) the sensitivity of the electrode, with its low roughness factor, to poisoning by impurities (this is minimized by the high electrode potential at which O_2 is reduced and by the continuous surface renewal due to the small corrosion current present in most cases); (b) the low concentration of surface peculiarities which are abundantly present in the very rough surface of porous electrodes and which may have enhanced activity for the electro-reaction; and (c) the difference in electrode structure from the structure of the practical electrode.

This combination of advantages and disadvantages necessitates using this method as a test for corrosion rate (with and without forced convection), and as a screening test for indications of O_2 -activity on materials which show reasonable corrosion resistance; this method will also be used for a more detailed study on mechanisms of O_2 -reduction on selected materials. Simultaneously, we plan to examine materials which show promise either from the rotating disc experiments or from previous experiences and literature data. This will be accomplished by mixing these materials with a hydrophobic binder and testing them as a half cell in a floating electrode setup (described below). Finally, exceptionally active materials will be tested in complete fuel cells.

II. EXPERIMENTAL METHODS

This section describes the procedures now in operation for the preparation of the ingot, the mounting of the sample as a rotating disc electrode, and the actual testing of this sample. The results on several materials tested by this method are summarized in Section III.

In addition, a technique of examining half cell electrodes which previously have been shown to yield consistent results is described. This apparatus has been built, but no experiments have yet been made.

A. Testing of Solid Ingots as Rotating Discs

Preparation of the Disc Electrode

1. Carefully weighed mixtures of pure elements are arc-melted in a furnace with six water-cooled copper heaters (each one-inch in diameter) using a tungsten tip under an argon atmosphere. A Ti getter is fired before each run in order to eliminate traces of O_2 . A maximum of six ingots weighing 5 to 10 grams can be obtained in one run.

2. If the alloy or compound is formed peritectically (i. e. during the solidification, the composition of the solid phase differs from the composition of the liquid phase) the ingot has to be annealed, preferably overnight at a convenient temperature. If the alloy or compound is formed congruently (i. e. the solidifying phase always has the same composition as the molten phase) this ingot can be used without any subsequent thermal treatment.

3. The ingot has a button shape when removed from the furnace and has to be cut with a boron carbide or chromonel saw in order to expose two parallel flat circular faces (see Fig. 1).

4. One part of the sawed button is used for metallographic analysis, according to standard procedures.

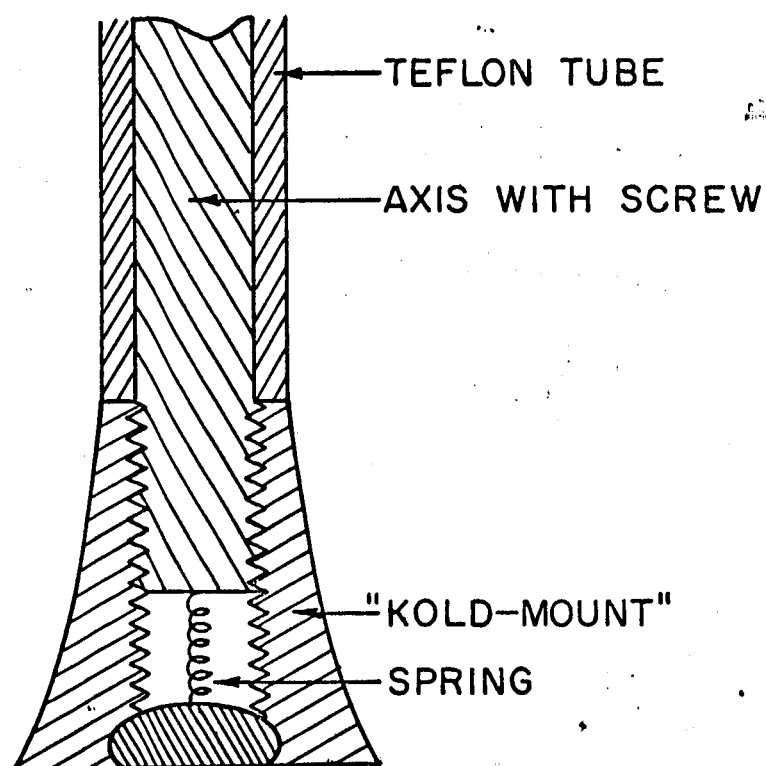


Fig. 1

ROTATING DISC ELECTRODE

5. The part of the button with the two parallel flat circular planes is incorporated as shown in Fig. 1 with "Koldmount" (a resin used for metallographic work, which we have found to erode less than 0.05 mg/cm^2 in 2 N KOH at 80°C over a period of 80 hrs.) This arrangement, besides isolating the electrical contact to the electrode from the electrolyte, also constitutes an ideal configuration for controlling precisely mass transport to the electrode.

6. Electrical contact with the button is achieved by screwing a metal stirring rod down on a spring-loaded contact in the threaded shaft of the Koldmount. For protection against the electrolyte, the rod, spring, and contact are gold plated and the rod is covered with heat shrinkable Teflon tubing (see Fig. 1). The electrode assembly is mounted in a Sargent 600 rpm synchronous motor designed for voltammetry with solid electrodes. Contact between the stirring rod and the fixed lead is made by dipping a wire into a pool of mercury in the hollow top of the rod.

B. Electrochemical Testing

The Cell

The cell as shown in Fig. 2 is used. In this cell all the frits have been eliminated since they disintegrate in caustic solution. The lack of a frit between working and reference electrodes does not introduce a significant error, since during the cathodic oxygen reduction (with oxygen saturated solution) only oxygen is evolved at the counter electrode. The hydrogen evolved at the counter electrode during the corrosion test (N_2 -saturated solution) which may dissolve and reach the working electrode is largely swept away by nitrogen, and therefore does not contribute significantly to the measured current.

The temperature of the cell is regulated $\pm 0.5^\circ\text{C}$ by using a heating mantel and a regulator with a temperature sensor inside the electrolyte. As a base line a temperature of 75°C has been selected for the experiments.

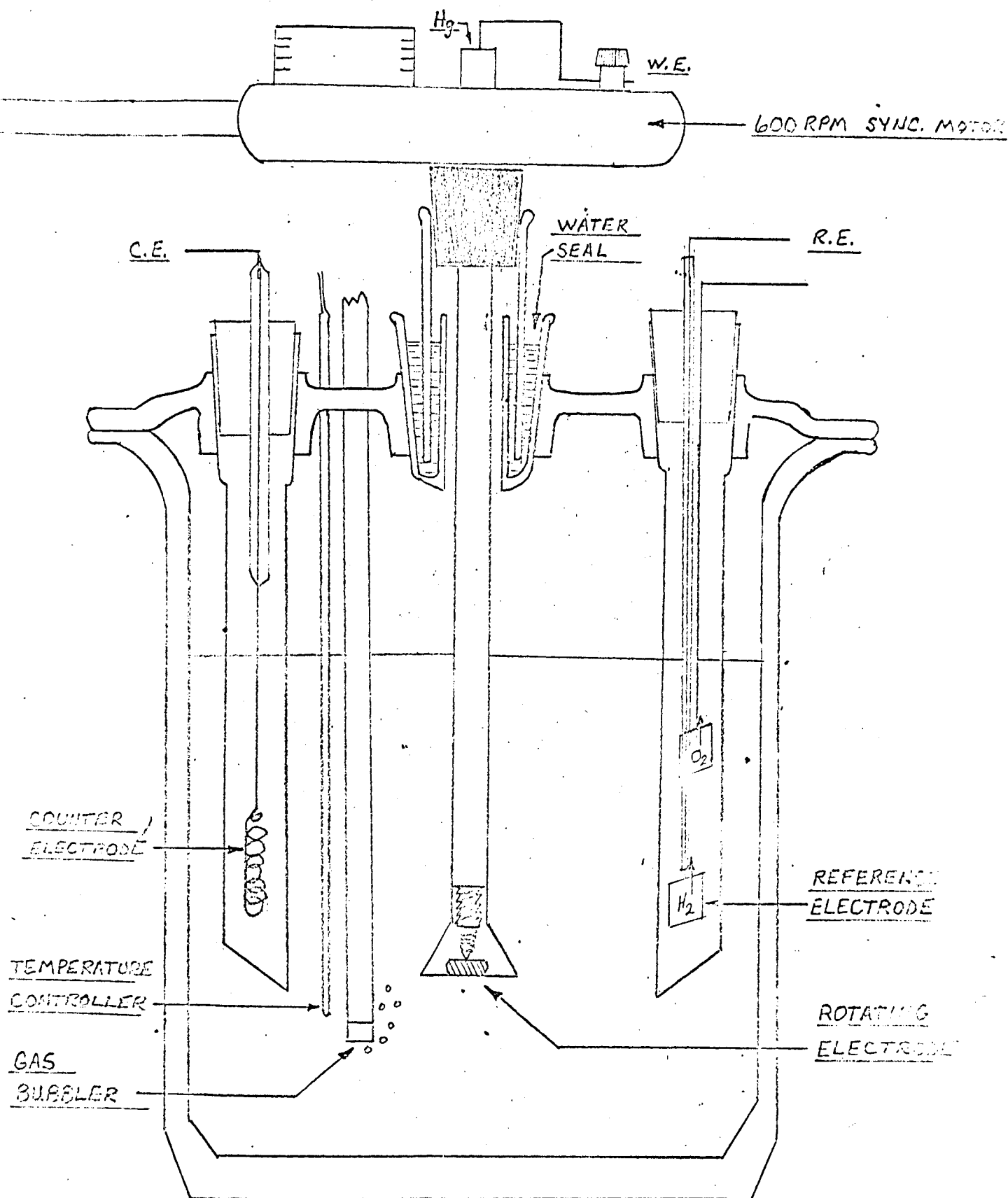


Fig. 2

ROTATING ELECTRODE CELL

All the experiments reported have been done using only one cell. A second cell has been built and will be used in parallel, in order to utilize better the electronic instrumentation and the available time, since extended periods are consumed with deaeration, repolishing the samples, etc.

The electrolyte concentration has been set at 2 M KOH after preliminary experiments with 35% (8.4 M) KOH (see "Results"). This concentration has a more favorable transport factor ($D \times C$) than 8.4 M KOH solutions used in practical fuel cells. Since the screening electrolyte is milder than practical conditions, the chances of missing a possible catalyst are reduced. However, favorable results obtained with 2 M KOH solution have to be extended to higher concentrations by subsequent tests.

Electrochemical Measurements

i (E)-curves are generated by imposing a linear potential scan on the working electrode by means of a slow linear potential signal to a Wenking potentiostat. The slow function generator was constructed with two standard batteries, two 10 turn, 10 K potentiometers, and a synchronous motor (InSCO Corp., Groton, Mass.). The motor has a basic speed of 4 rpm and six gear ratios of 1:1, 2:1, 5:1, 10:1, 20:1 and 50:1. By changing these gear ratios and the peak voltage, scanning rates from 10 mv/min to 800 mv/min can be obtained. For the initial routine screening, a rate of 50 mv/min has been selected.

The current-potential curve is recorded directly on an x-y recorder. Current-time curves at constant potential for relatively long times can be recorded on the same recorder by using the slow function generator to feed the y-axis of the recorder.

Before an activity test experiment, the corrosion current under inert gas (N_2) is measured at a series of potentials. This corrosion current has to be measured with stirring in order to subtract it quantitatively from the O_2 reduction current. It is also measured without

stirring in order to apply the results to a practical electrode. Also the possibility of corrosion decrease with time has to be investigated. As long as the corrosion current is small compared with the expected O_2 -current ($i_L = 2 - 4 \text{ ma/cm}^2$) the O_2 -curve will be run, even if the corrosion rate is higher than useful for a practical cell.

In order to ascertain whether an observed performance represents an intrinsic activity of the compound and not a mere increase of the surface area, the real surface area of the electrode has to be estimated. The only practical method of doing this during screening of a large number of flat electrodes is by measuring the double layer capacity of the electrode.

For the capacity measurements, we have selected a method in which a triangular wave of 50 cycles/sec and a peak-to-peak voltage of 100 mv (i. e. a sweep rate of 10 volts/sec), biased by a convenient dc voltage, is fed to the signal input of the potentiostat. The dc voltage is selected so that faradaic currents are avoided. If the electrode behaves as a perfect capacitor (no faradaic or ohmic resistance) the small triangular potential wave is transformed into a square current wave, with a peak-to-peak value which is proportional to the electrode capacity and therefore to the real surface (see Appendix B).

Procedure

The following procedure is being used at the present for routine screening. Modifications of the procedure will be introduced when advisable.

1) N_2 Saturation: A freshly prepared 2 M KOH solution is saturated with pure nitrogen for at least 45 minutes. The electrode is kept inside the cell but not exposed to the electrolyte until N_2 saturation is complete.

2) Corrosion $i(E)$ Curve: The electrode is introduced into the solution at a potential of $E = 0 \text{ mv}$. The potential scan is initiated within a minute at a rate of 50 mv/min and 600 rpm rotation.

The potential scan is reversed between $E = 0.8$ volt and $E = 1.23$ volts, depending on the extent of corrosion in this range. If there is a high corrosion rate at the lower potentials, higher potentials are still investigated since there may be a region of passivation in the potential range of interest.

At several points of the $i(E)$ -curve, stirring is stopped for 1 or 2 minutes without stopping the potential sweep (in order to see the effect of stirring on corrosion).

3) Measurements of the Double Layer Capacity: At several points in the $i(E)$ -curve (under N_2) the recording is interrupted and a double layer capacity measurement is made as described above.

The electrode potential is never left uncontrolled in order to control the history of the electrode from the moment it is immersed in solution. If, in addition to the $i(E)$ -curve, the electrode has to be left for some time at a known potential, the time at this potential is kept as short as possible and noted. During extended periods of inactivity the electrode is removed from the solution and any attached electrolyte is removed by rotating the electrode in the gas phase for a short time (for instance, half a minute).

4) O_2 -Saturation: If the corrosion current is within tolerable limits, the test for O_2 -activity is carried out. The electrode is removed from the system and repolished, and the solution is saturated with O_2 (at least $3/4$ hour).

5) $i(E)$ -Curve for O_2 -Reduction: The repolished sample is introduced into the electrolyte at a high, passive potential when possible, but below any current wave (usually between 0.8 volt and 1.23 volt) and the $i(E)$ -curve is initiated in the direction of the decreasing potentials. At $E = 0$, the direction of the potential sweep is reversed.

6) To eliminate the effect of poisoning it may be advisable in a few cases to repeat some $i(E)$ -curves with different potential sweep rates ranging from 20 mv/min to 400 mv/min.

7) Measurement of the double layer capacity in the region of the limiting current may be necessary when doubts exist about real surface increase incurred during the recording of the $i(E)$ -curve.

8) After recording the $i(E)$ -curves a micrograph of the electrode surface is taken and the sample is filed for subsequent study.

C. Testing of Finely Divided Catalysts

Materials showing negligible corrosion and some degree of O_2 -activity in the previous test, or materials which are known from previous experience (including literature) for activity in O_2 -reduction will be tested as finely divided powders. These will be prepared by any method yielding fine powders such as pulverizing of solid ingots, co-precipitation (with the reservations expressed in the introduction), plasma spraying, explosion of wires, thermal decomposition of salt mixtures, etc. After preparation, the real surface of the resulting finely divided material will be measured using the B. E. T. krypton adsorption system.

The electrode will be made by mixing the material with a suitable amount of Teflon powder (Teflon - 30) or with polyvinyl resin, sintering or drying, and bonding to a fine mesh Ni-screen for electrical contact.

The electrode will be tested in a "floating electrode"* system which is already fabricated and operable (see Fig. 3). This cell consists of an electrode ($\sim 1 \text{ cm}^2$ area) placed on the surface of the electrolyte over which reactant gas is passed. This simulates the operation of a half cell without the complications of cell construction and operation in a contained electrolyte. In addition the time required for characterization with O_2 is about 1/2 hour, a considerable saving.

* J. Giner and S. Smith to be published.

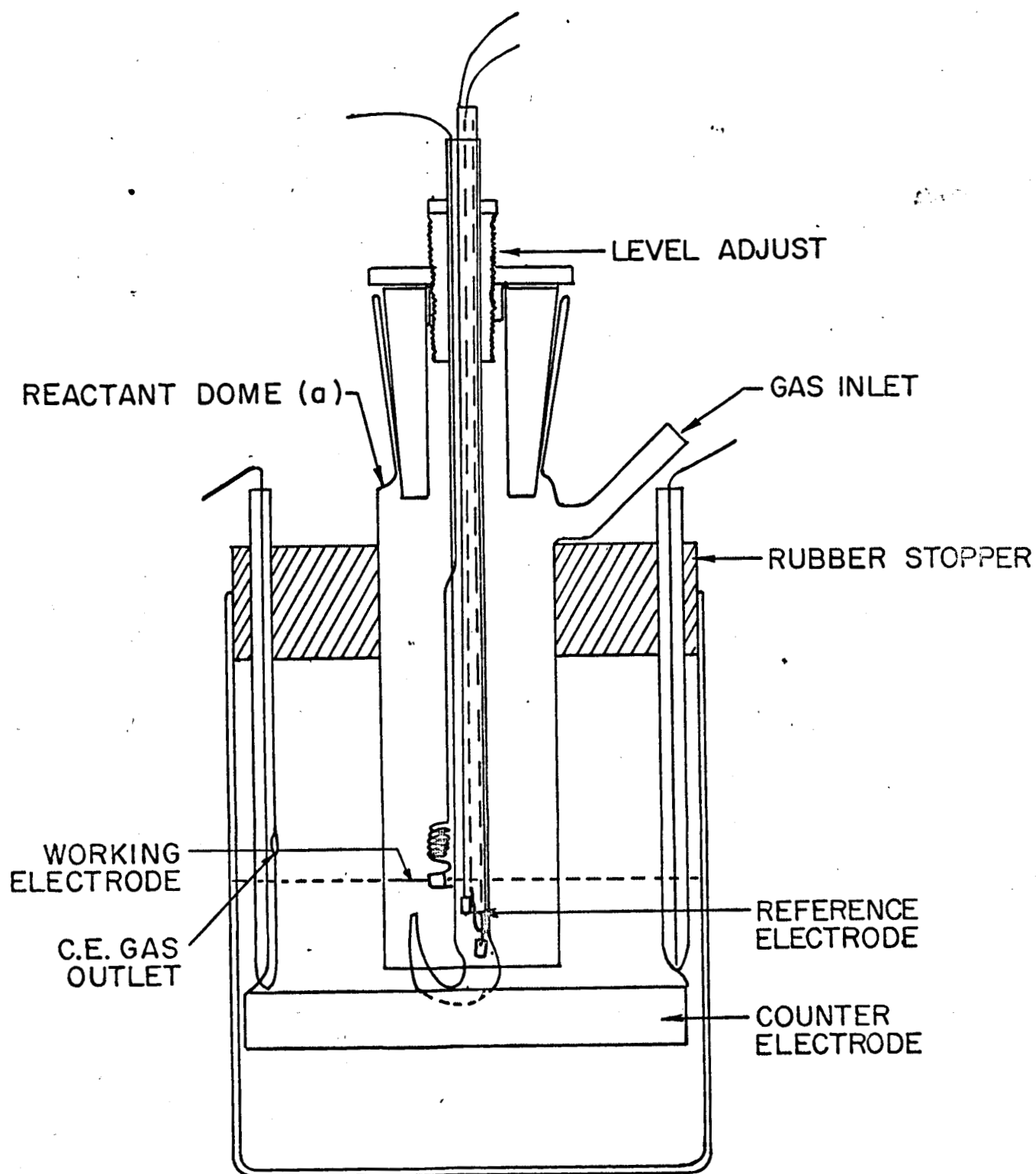


Fig. 3

FLOATING ELECTRODE CELL FOR THE MEASUREMENT OF ACTIVITY
OF HYDROPHOBIC POROUS ELECTRODES

The body of the cell is a 500 ml resin reaction kettle. The cover supports the working electrode, reference electrode, and gas inlet. The gas exits from the cell through the threads in the level adjust screw. The reference electrode and the working electrode holder are made in one piece so that the capillary tip is always at the same distance from the electrode. With this arrangement the resistance included in the electrode potential measurement is a constant for a given electrolyte and need be measured only once for a series of determinations in a given electrolyte. This is a distinct advantage, since it is very difficult to place the capillary tip in such a position with respect to the working electrode that a constant or zero iR drop will be included in the polarization measurements, if the distance is adjusted with each electrode.

The electrode holder is fitted into the center tube with a screw device which permits a fine control on the level of the electrode with respect to the electrolytes and permits the electrode to be accurately placed in the solution. Using this device it was found that raising or lowering the electrode from a position level with the electrolyte surface by 3 mm made less than 2% change in the current and thus the elevation of the electrode with respect to the solution is not critical.

III. RESULTS

The following intermetallic compounds and alloys have been melted thus far in the program:

Cr_3C_2	Nb_3Pt	TaV_2	TiNi_3
		TaIr_3	Ti - 81 at % Cr
Cr_3Pt	NbPt	Ti_3Au	$(\text{Ti}, \text{Zr})\text{Cr}_2^*$
	Nb - 47.5 at % Re		
HfC	Ni_3Cb	TiC	WC
Hf_2Pt	NiZr_2	TiCo	W_2Hf
MoNi	Ta_2Ni	TiCr_2	Zr_2Au
MoNi_3	TaNi	Ti_2Cu	ZrAu_3
MoNi_4	TaNi_2	TiCu	ZrAu_4
Mo_3Pt	TaNi_3	TiCu_3	ZrC
NbC	TaPd_3	Ti_2Ni	ZrNi_5
Nb - 37.5 a/o Pt	TaPt_2	TiNi	Zr_2Pd
(σ phase)			ZrPd_2
Nb + 75 at % Re			
X phase			

In addition, carbides of Nb, Ta, Mo, W, Cr, Ti, Zr, and Hf are available as (- 325) mesh powders.

All of these compounds and alloys cannot be immediately tested for corrosion, since some of these form via a peritectic reaction, and must be heat treated in order to attain a single phase compound. Those

* 21.6 a/o Ti, 15.0 a/o Zr, 63.4 a/o Cr

compounds which form congruently may be tested as soon as the particular ingot has been cut and metallographically prepared. The primary emphasis now is to work with those compounds which form congruently.

The results for corrosion and oxygen reduction obtained this far are given in Table I and Figs. 4 - 24. Only a brief discussion of the results is given here. A more extended analysis will be carried out later.

A. Behavior of Pure Metals

Pure metals with known catalytic behavior for the reduction of O_2 , such as Pt, Ag, and Au have been tested in order to confirm the applicability of the method and to establish some standards of comparison under the same testing conditions. In addition, testing has been started with other elements in order to compare their behavior (corrosion and O_2 -activity) with that of the alloys.

Platinum (Fig. 4): The electrochemical behavior of Pt has been the object of numerous studies; therefore this metal can be taken as a standard. The $i(E)$ -curve shows no activity above 1.0 volt, and below this potential the current increases sharply with increasing polarization. This agrees well with the results obtained with porous electrodes. The lack of activity and the hysteresis in the activation controlled section of the curve can be explained by assuming that the Pt-O layer which covers the electrode almost completely at potentials higher than $E = 1$ volt is inactive for O_2 -reduction. As this oxide is reduced, the activity of the electrode increases sharply.

Gold: The $i(E)$ -curves of Fig. 5 show, in the first place, that at high KOH concentrations (35%, 8.4 Molar) the $i(E)$ -curve is not as well defined as with 2 M solution; this can be attributed to decreasing O_2 -solubility with increasing KOH concentration and these considerations have dictated the selection of the 2M solution for all

Table I

Comparison of Currents at Constant Voltage

Potential (mv)	N ₂ - Corrosion Current $\mu\text{a/cm}^2$			O ₂ - Reduction Current $\mu\text{a/cm}^2$			Differential Reduction Current $\mu\text{a/cm}^2$		
	900	800	500	900	800	500	900	300	500
Pt	Increasing	0	0	-45	-1310	-1680	567	1310	1640
	Decreasing	0	0	-45	-1310	-1720	454	1310	1680
Au	Increasing	+67	+67	+33	-501	-1430	0	568	1460
	Decreasing	+67	+67	+33	0	-1430	67	551	1460
Ag	Increasing	+40	+60	+20	-700	-1750	anodic	740	1770
	Decreasing	+40	+40	+10	-320	-1780	anodic	360	1790
Ta	Increasing	+60	+30	+25	+50	0	0	anodic	anodic
	Decreasing	+40	0	-10	+40	-40	0	anodic	-30
Zr ₂ Ni	Increasing	+680	+27	-137	-41	-410	13	68	273
	Decreasing	+27	0	-110	-41	-410	anodic	41	400
TiNi	Increasing	+762	+914	+927	+558	+127	153	305	800
	Decreasing	+178	+76	-406	-25	-762	38	101	356
NbPt	Increasing	+584	+571	+343	-952	-1460	864	1520	1800
	Decreasing	+152	+152	-13	-508	-1670	660	1490	1660
TiCu	Increasing	+486	+429	+944	+214	-114	167	215	1030
	Decreasing	+443	+343	+114	+371	-114	72	0	228

Table I (Cont.)

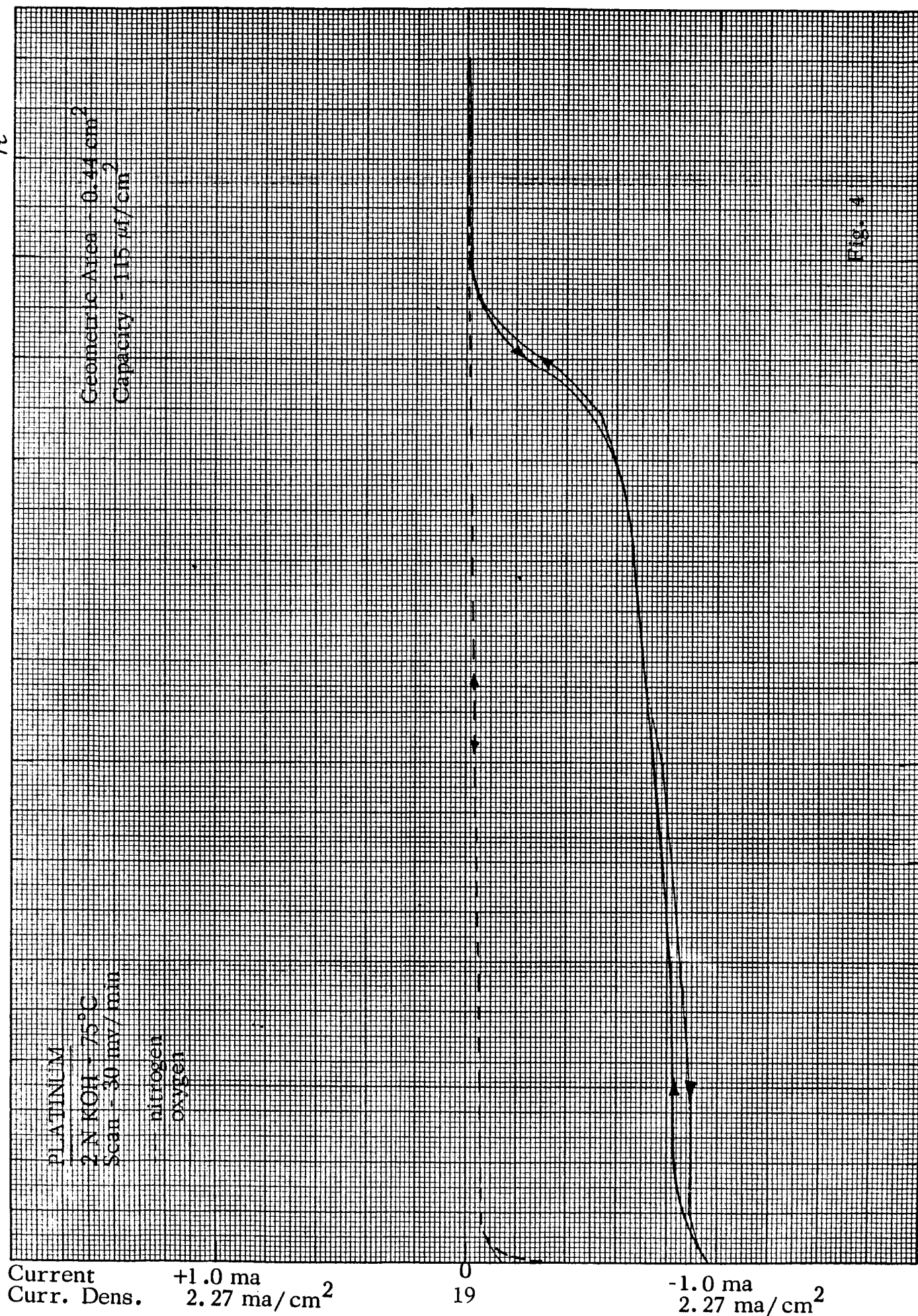
<u>Potential (mv)</u>		<u>900</u>	<u>800</u>	<u>500</u>	<u>900</u>	<u>800</u>	<u>500</u>	<u>900</u>	<u>800</u>	<u>500</u>
TaPt ₂	Increasing	+60	+51	0	-344	-912	-1100	350	963	1100
	Decreasing	+60	+51	0	-344	-912	-1080	350	963	1080
TiPt ₃	Increasing	+160	+120	-60	+560	-19	-195	anodic	760	1620
	Decreasing	+60	0	-140	-200	-20	-195	140	1400	2380
TaNi ₃	Increasing	+40	+40	+40	+340	+200	0	anodic	anodic	40
	Decreasing	+40	+40	+40	+340	+100	-100	anodic	anodic	140
TaPt ₃	Increasing	+414	+437	+287	+530	-805	-2110	anodic	1242	2400
	Decreasing	+115	+138	-92	-115	-920	-2300	230	1058	2210
TiCu ₃	Increasing	+1150	+2580	+575	+1350	+3500	-46	anodic	anodic	620
	Decreasing	+460	+345	+69	+805	+552	-46	anodic	anodic	115
ZrAu ₃	Increasing	+23	+23	+15.6	-78	-312	-2260	101	335	2280
	Decreasing	+23	+23	0	-78	-624	-2410	101	647	2410
NbNi ₃	Increasing	+80	+60	+10	+40	+10	-60	40	50	70
	Decreasing	+50	+40	-10	+30	0	-80	20	40	70
TiNi ₃	Increasing	+1740	+556	+230	+580	+11	-2320	1160	545	2550
	Decreasing	+46	-23	-556	-140	-278	-812	186	255	256
TiCr ₄	Increasing	+40	+40	+40	+40	+40	+40	0	0	0
	Decreasing	+40	+40	+40	+40	+40	+40	0	0	0
WC	Increasing	+750, 000	+175, 000	+8250						
	Decreasing	+520, 000	+130, 000	+5800						

Table I (Cont.)

<u>Potential (mv)</u>		<u>900</u>	<u>800</u>	<u>500</u>	<u>900</u>	<u>800</u>	<u>500</u>	<u>900</u>	<u>800</u>	<u>500</u>
TiC	Increasing	+1400	+500	+78	9300 $\mu\text{a}/\text{cm}^2$ at 1 volt in N_2					---
	Decreasing									---
Ni_3B	Increasing	+245	+210	+70	0	-105	-630	245	315	700
	Decreasing	+105	+52	-105	0	-105	-525	105	157	410

W. H. R. R.

pt



Au

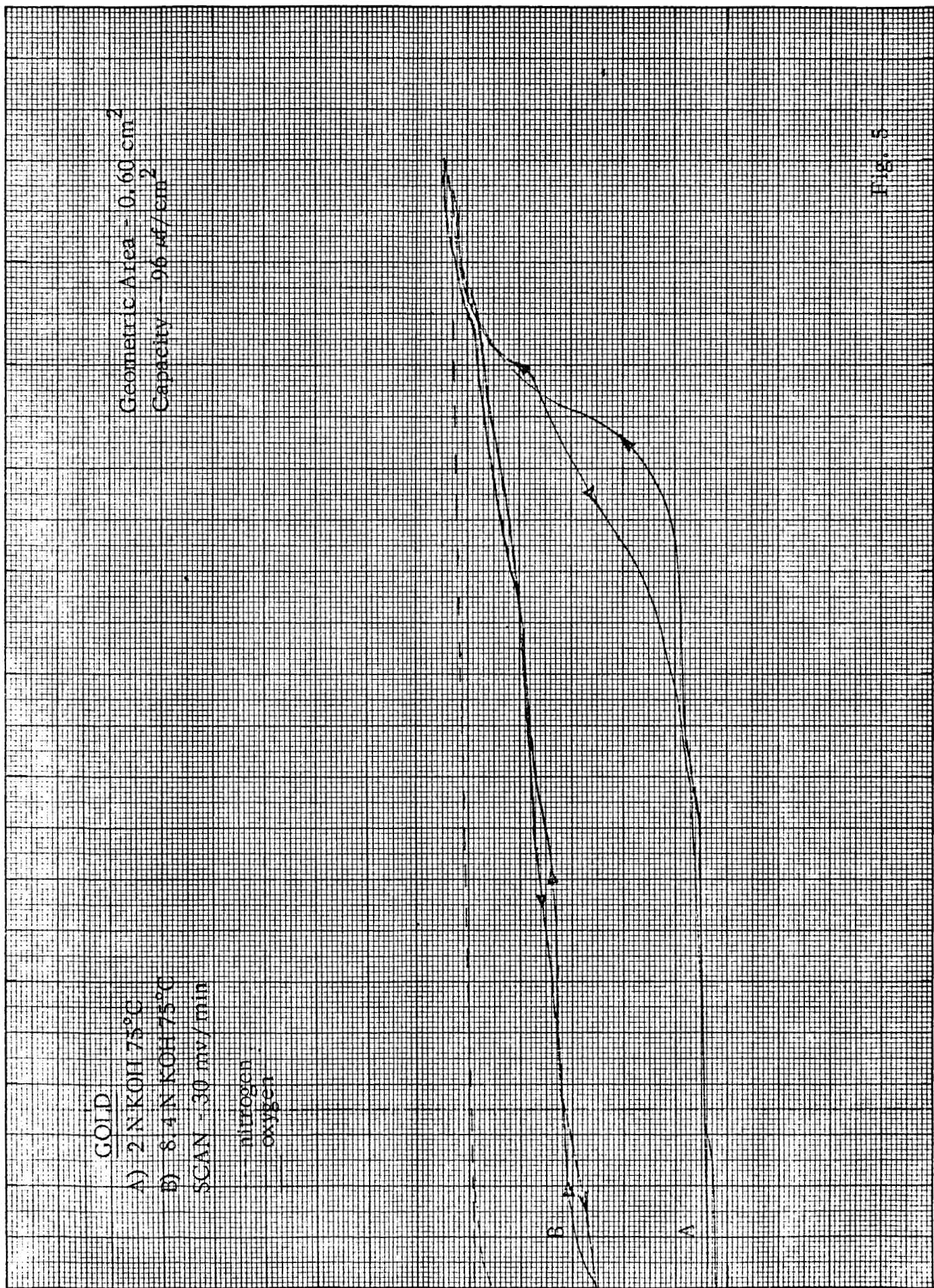
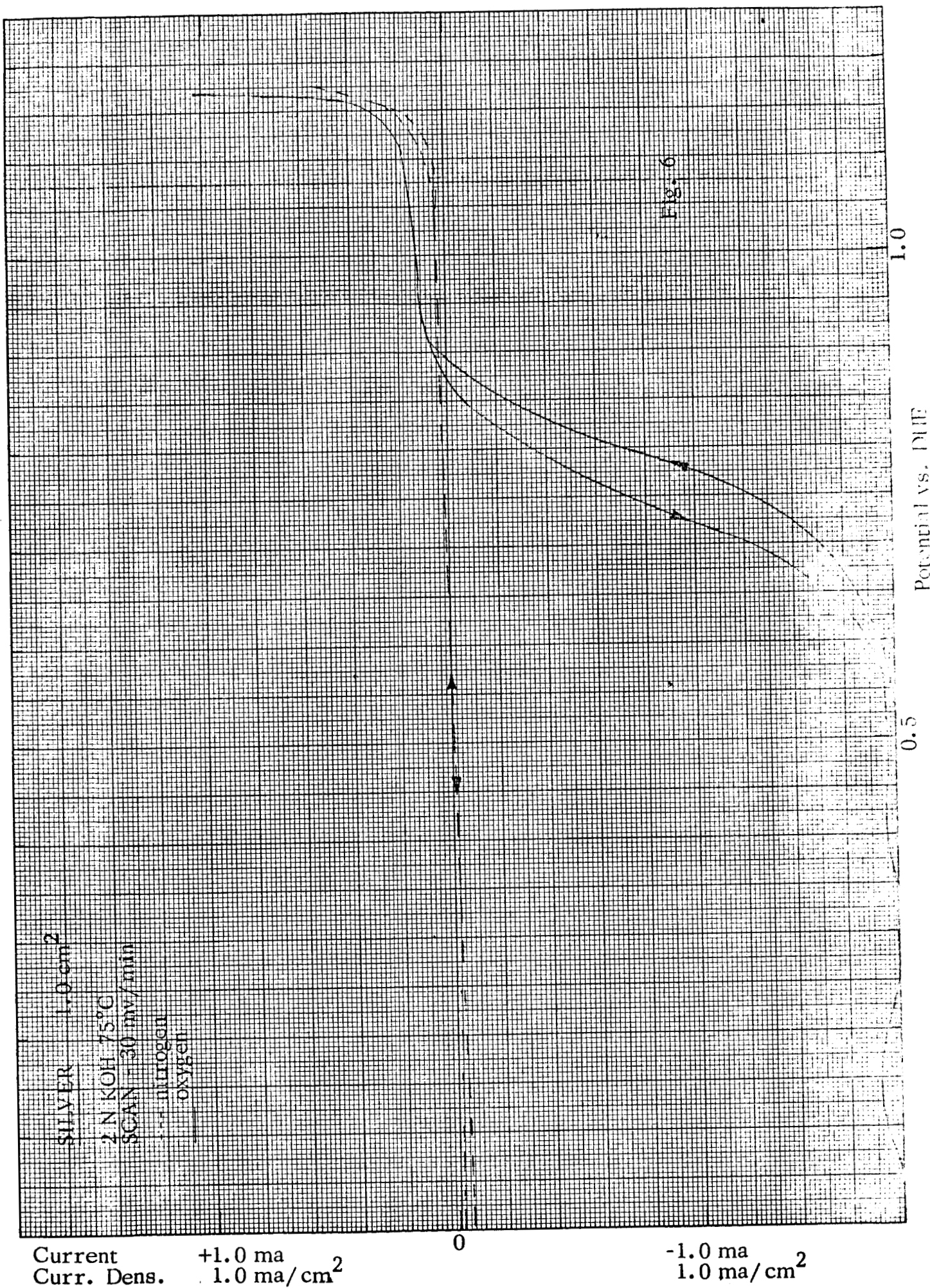
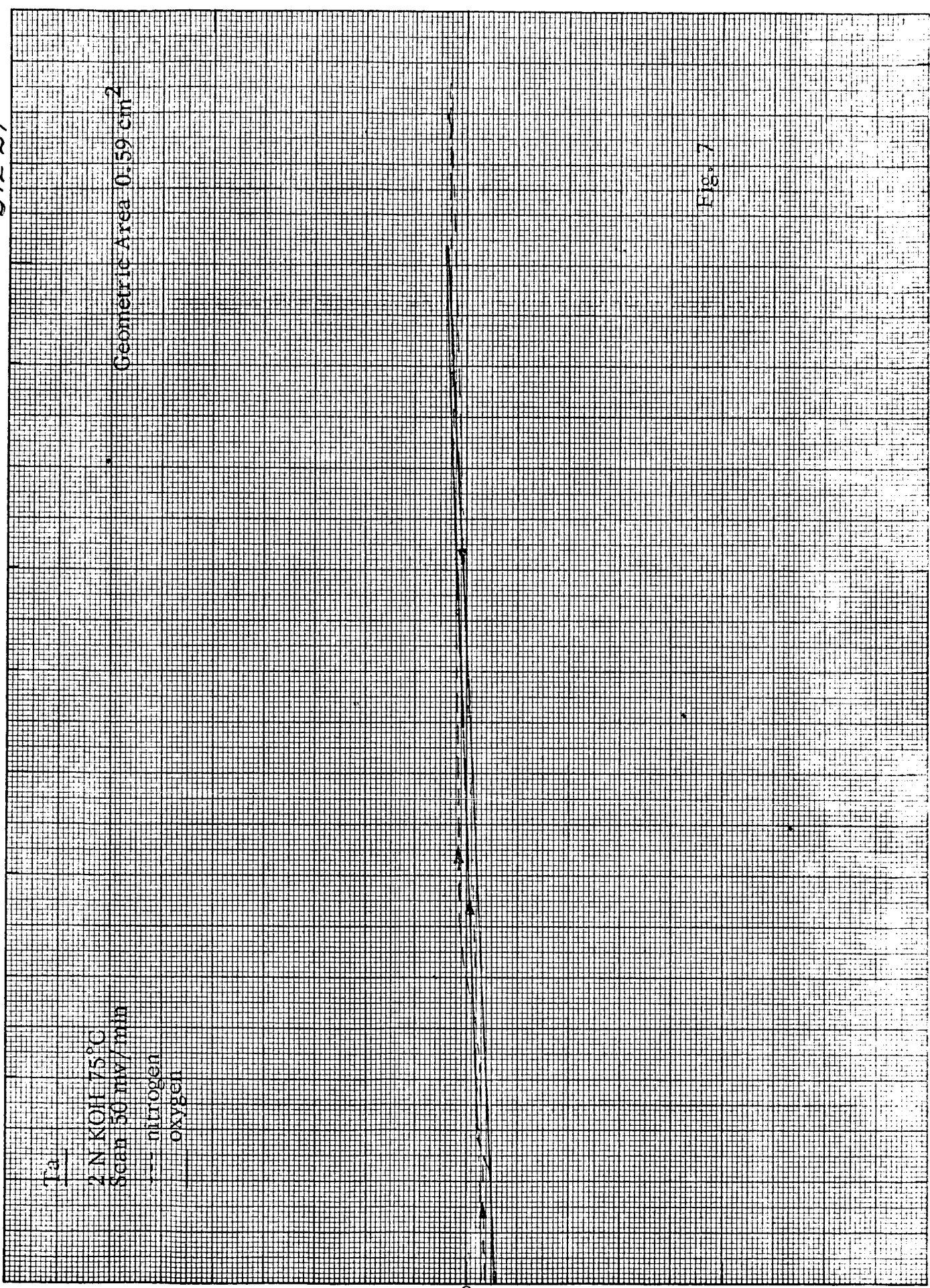


Fig. 5

Ag

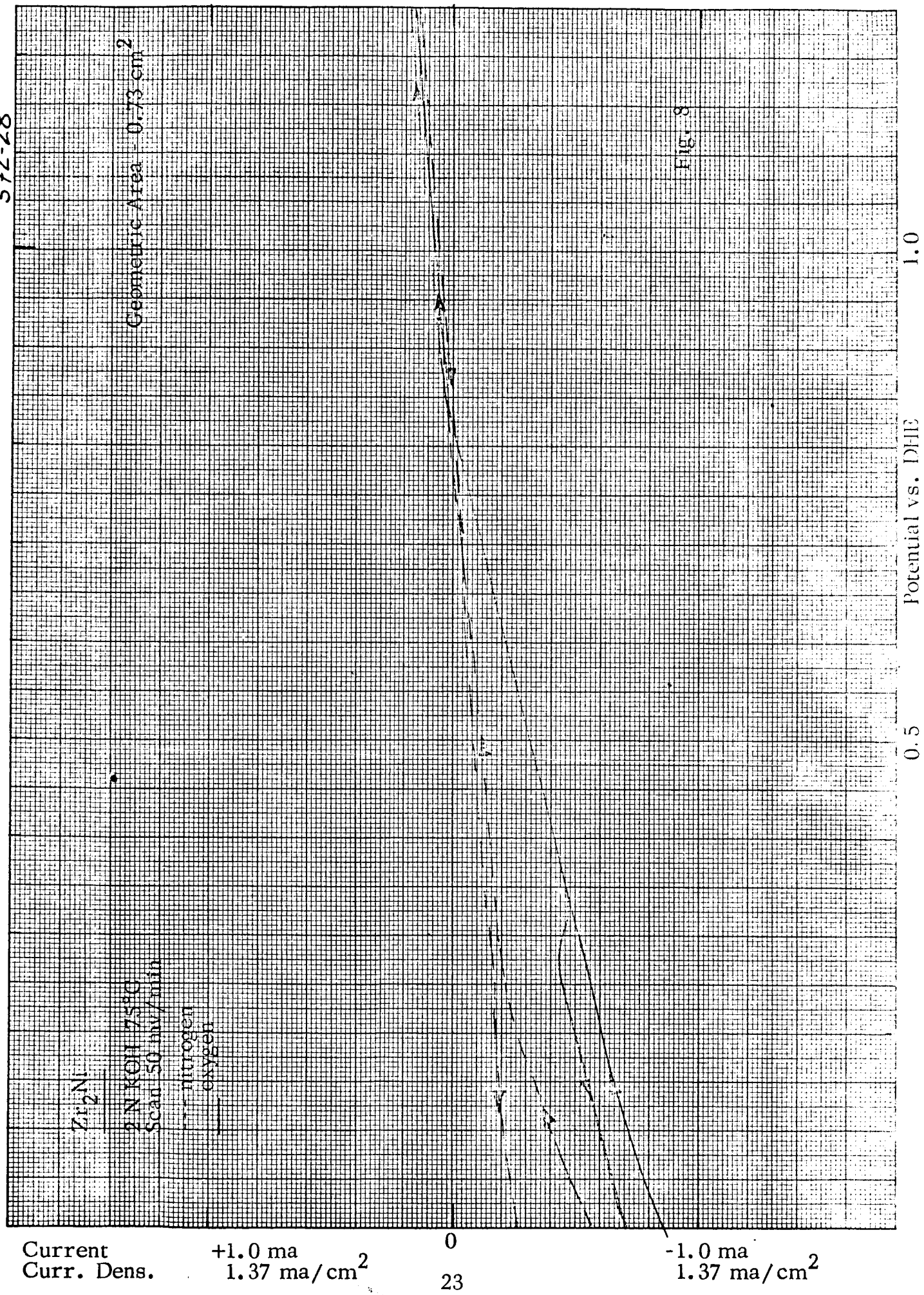


572-27

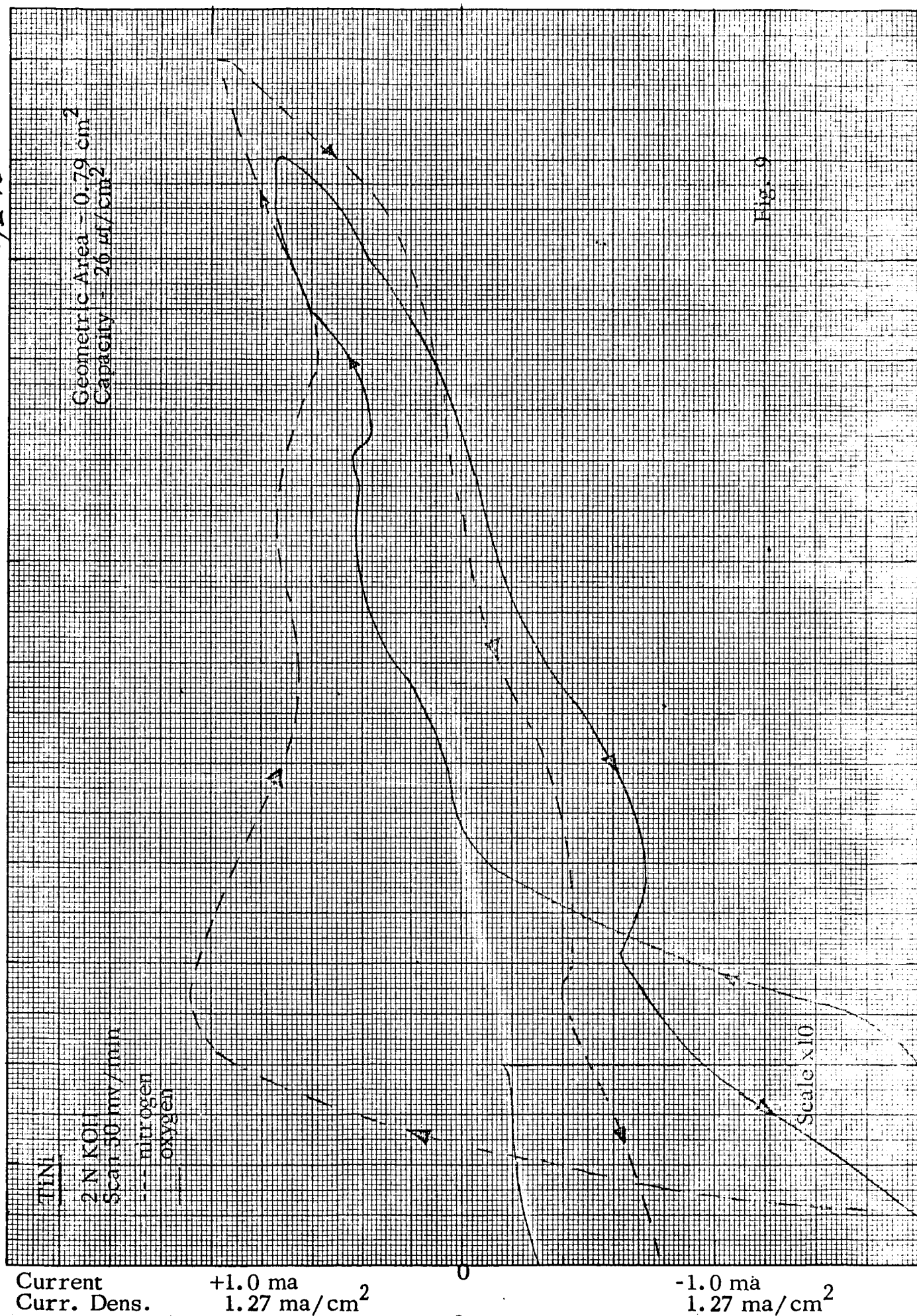


Current +1.0 ma 0 -1.0 ma
Curr. Dens. 1.7 ma/cm² 1.7 ma/cm²

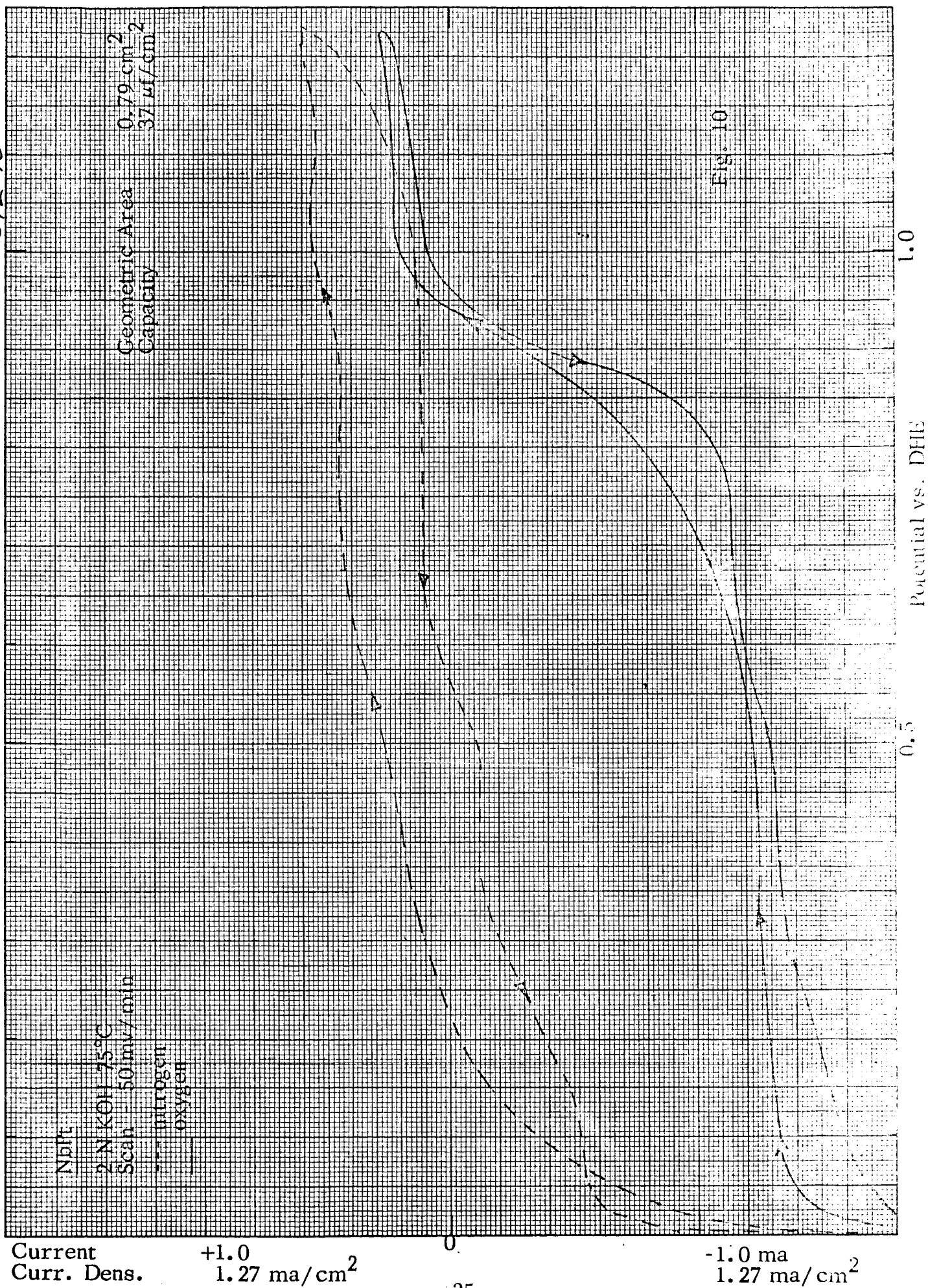
572-28



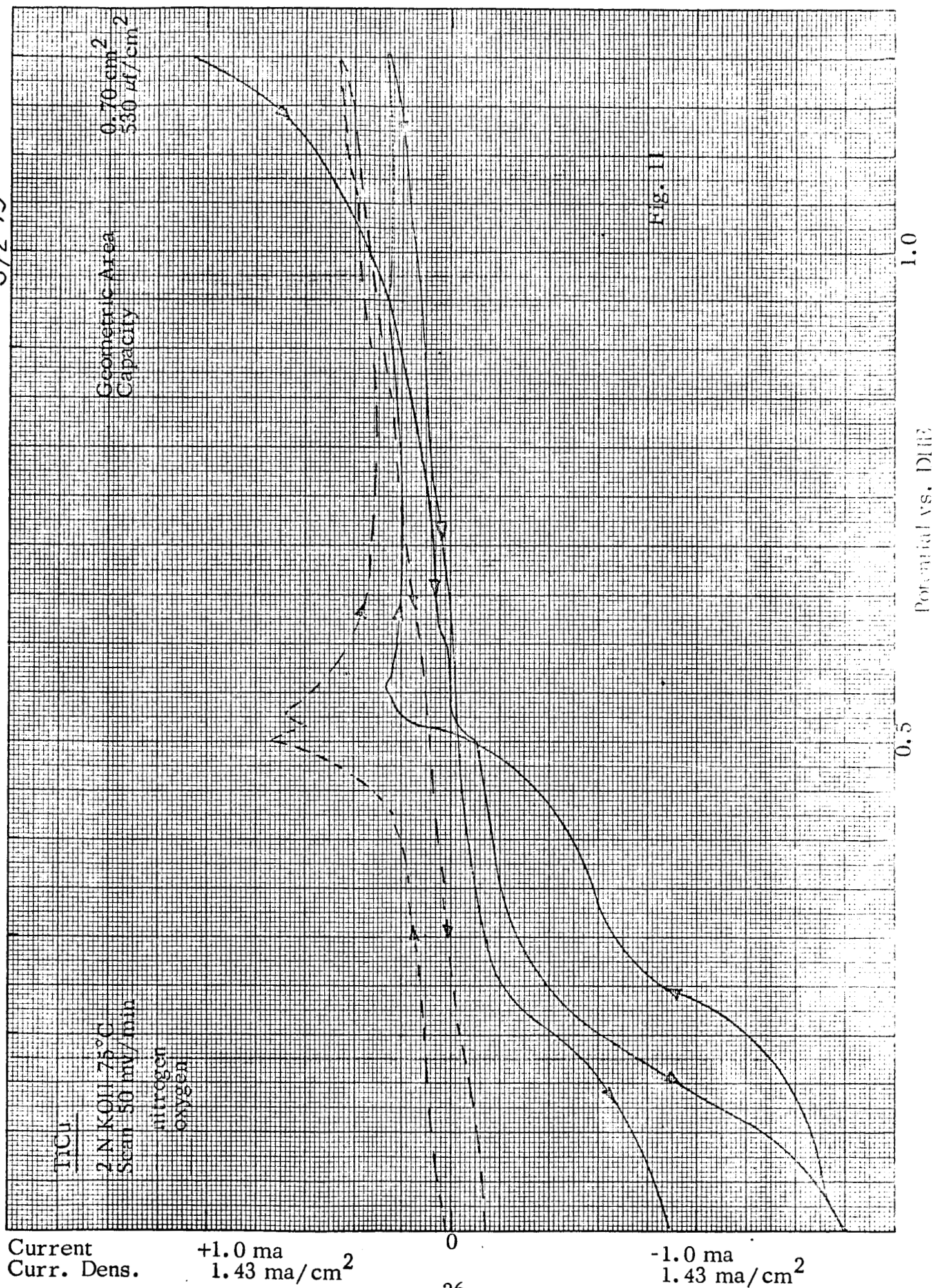
572-18



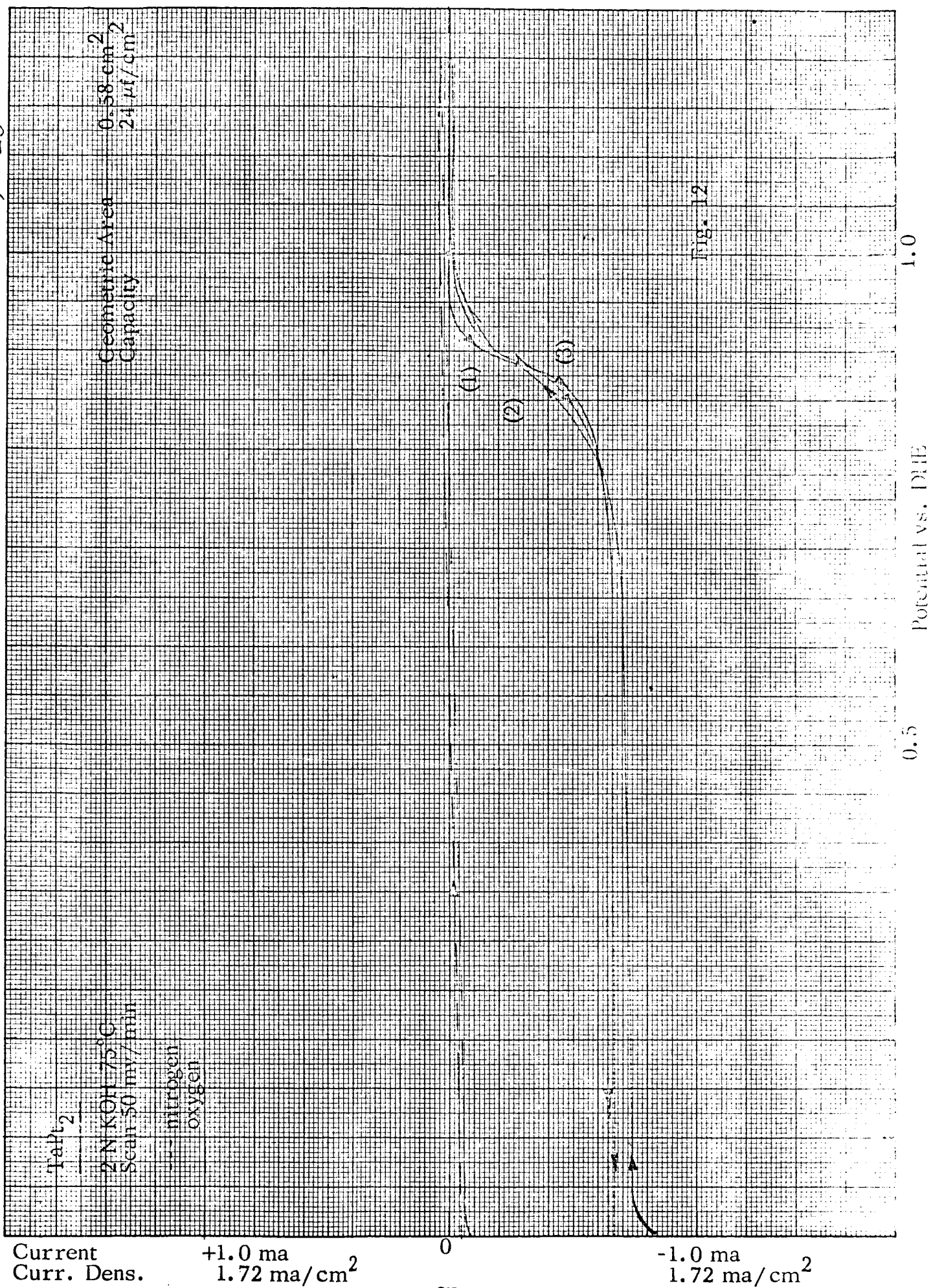
572-16



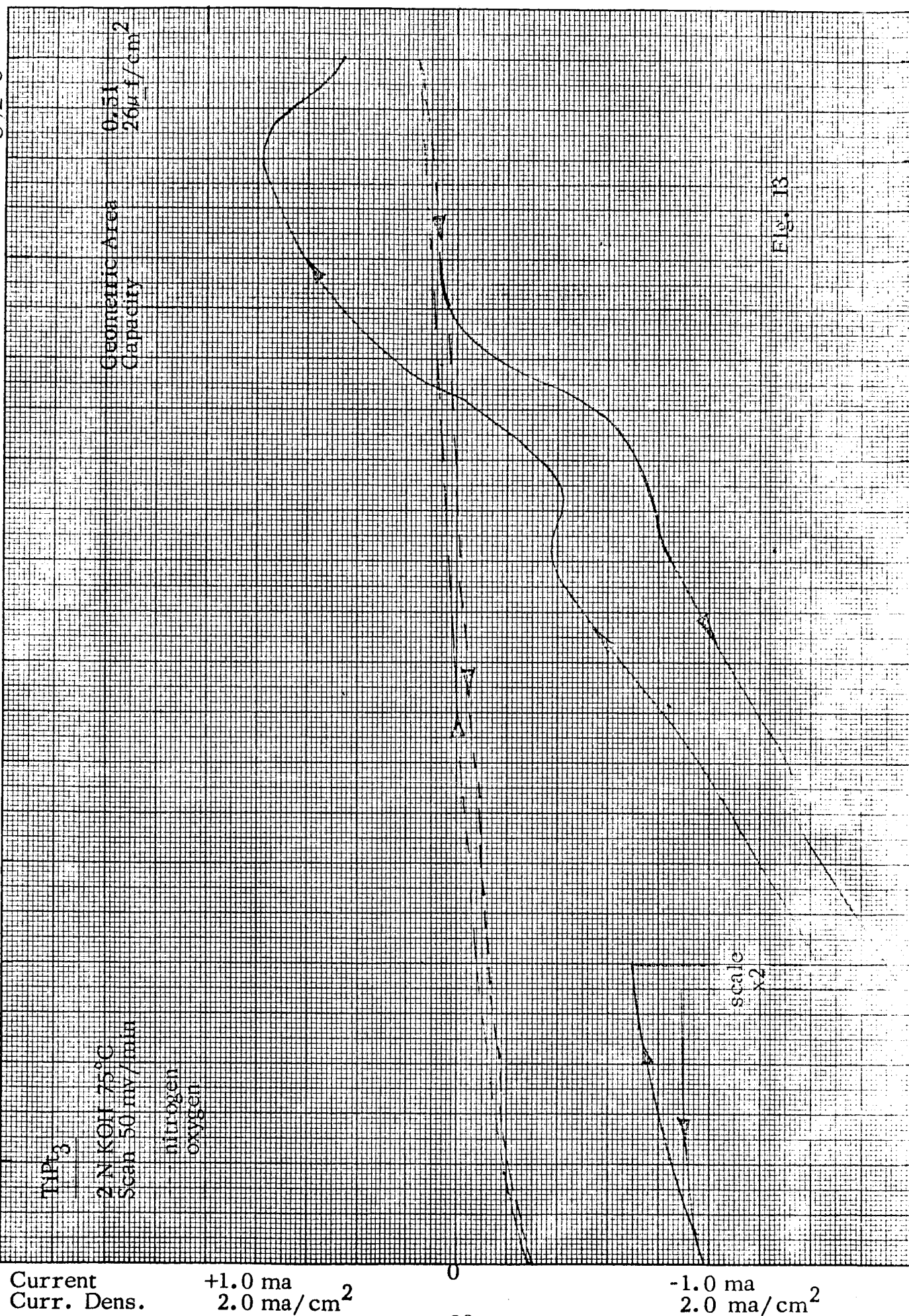
572-19



572-25

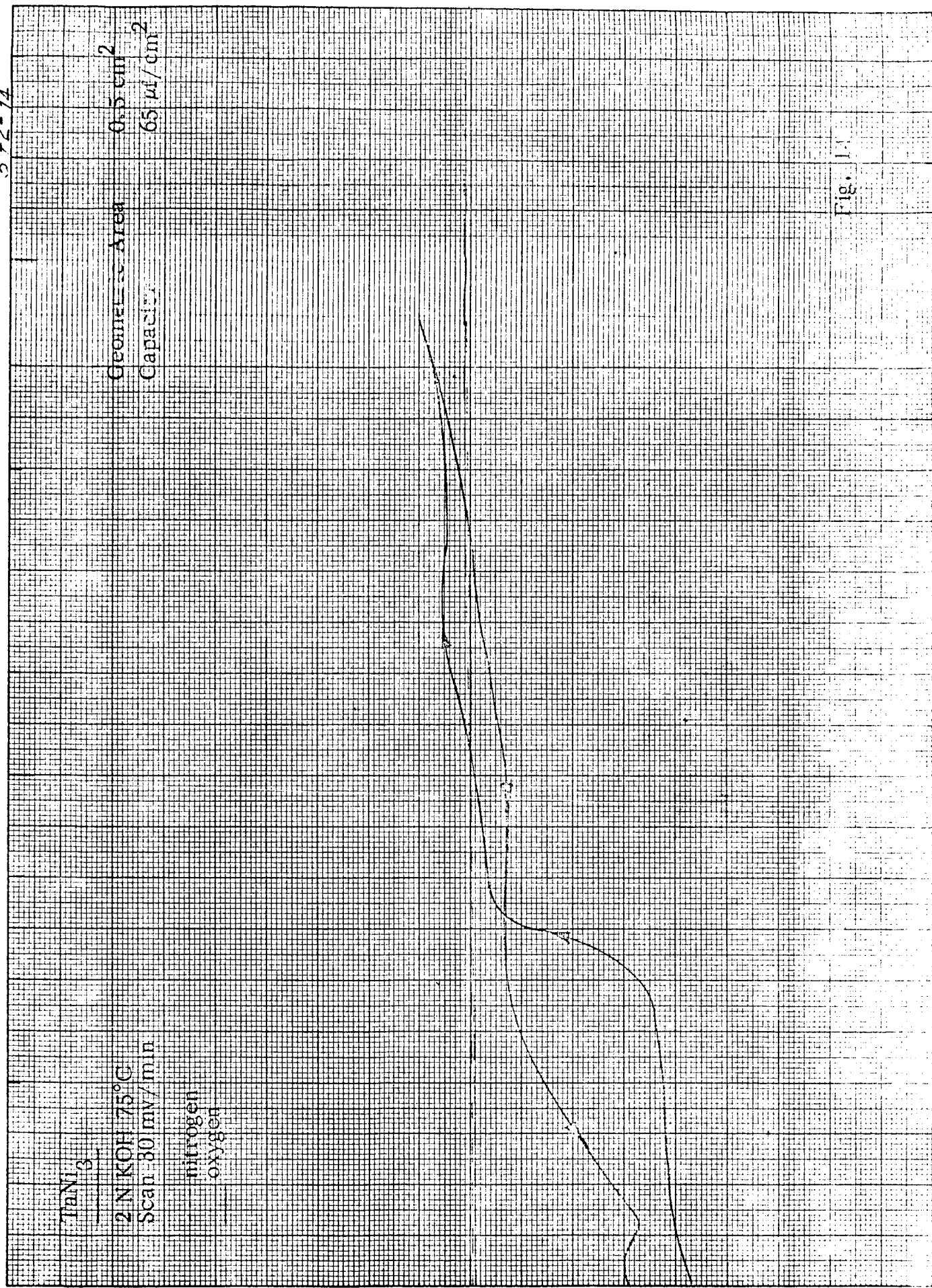


572-31

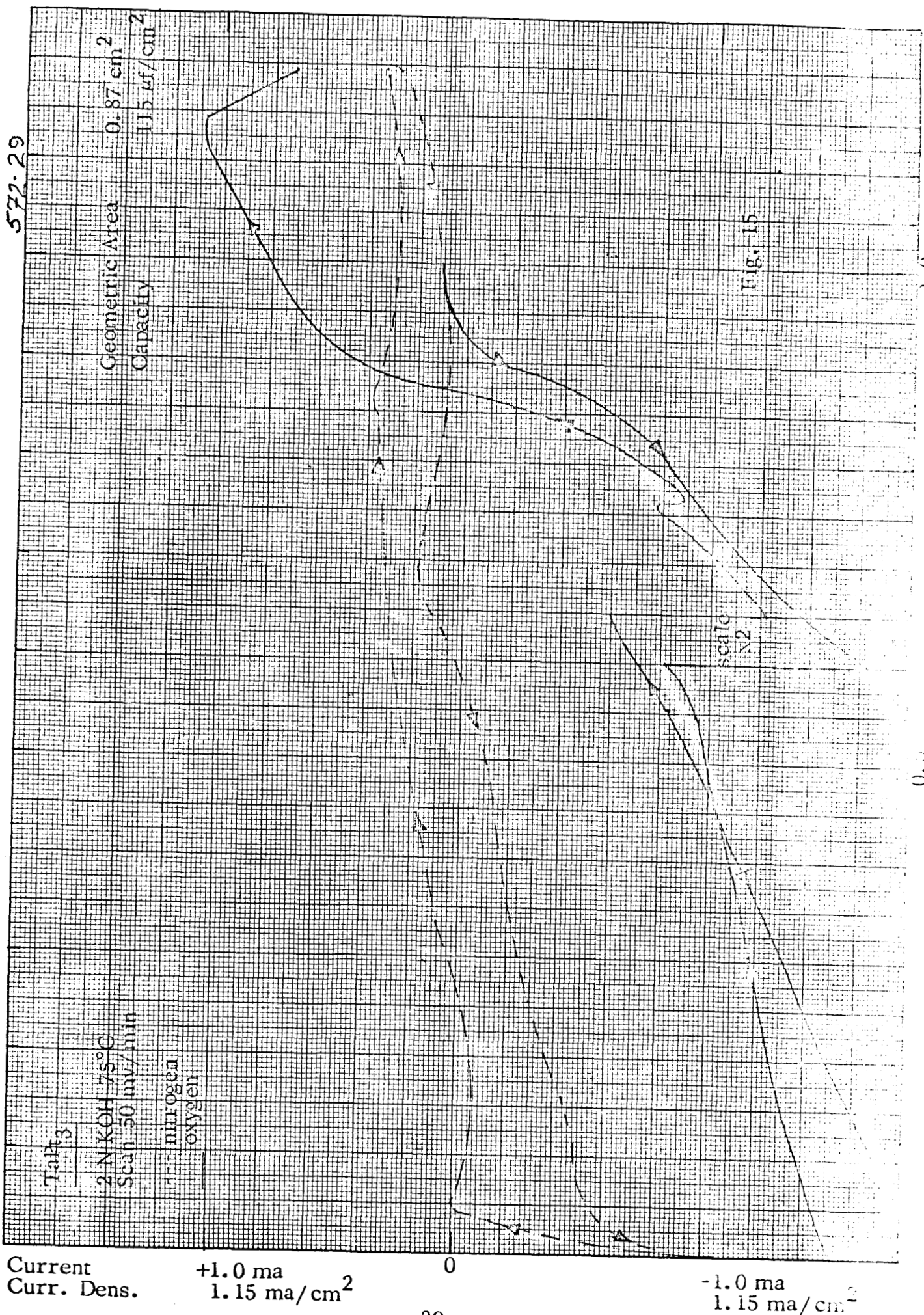


Potential vs. DHE 0.5 1.0

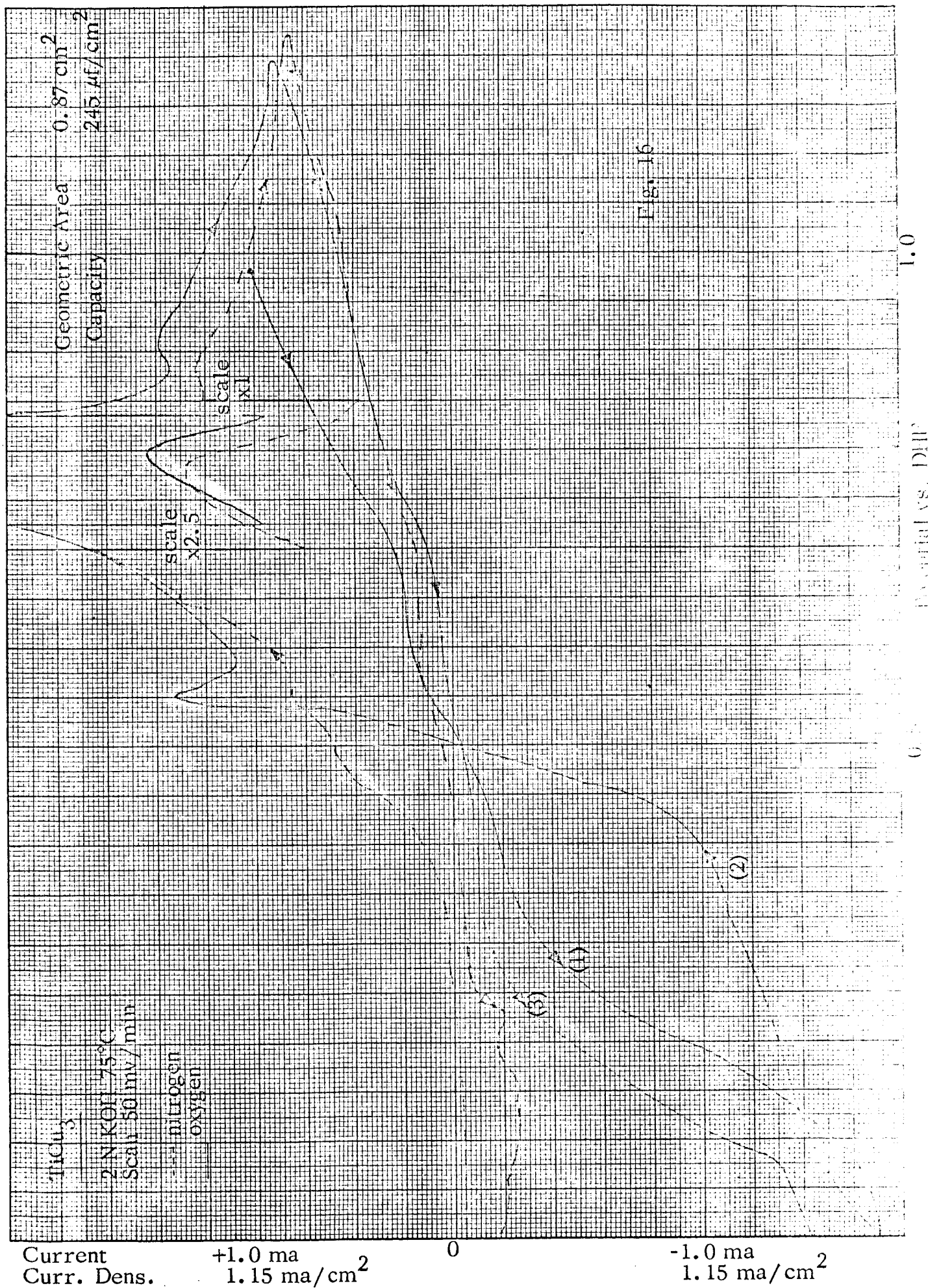
572-14



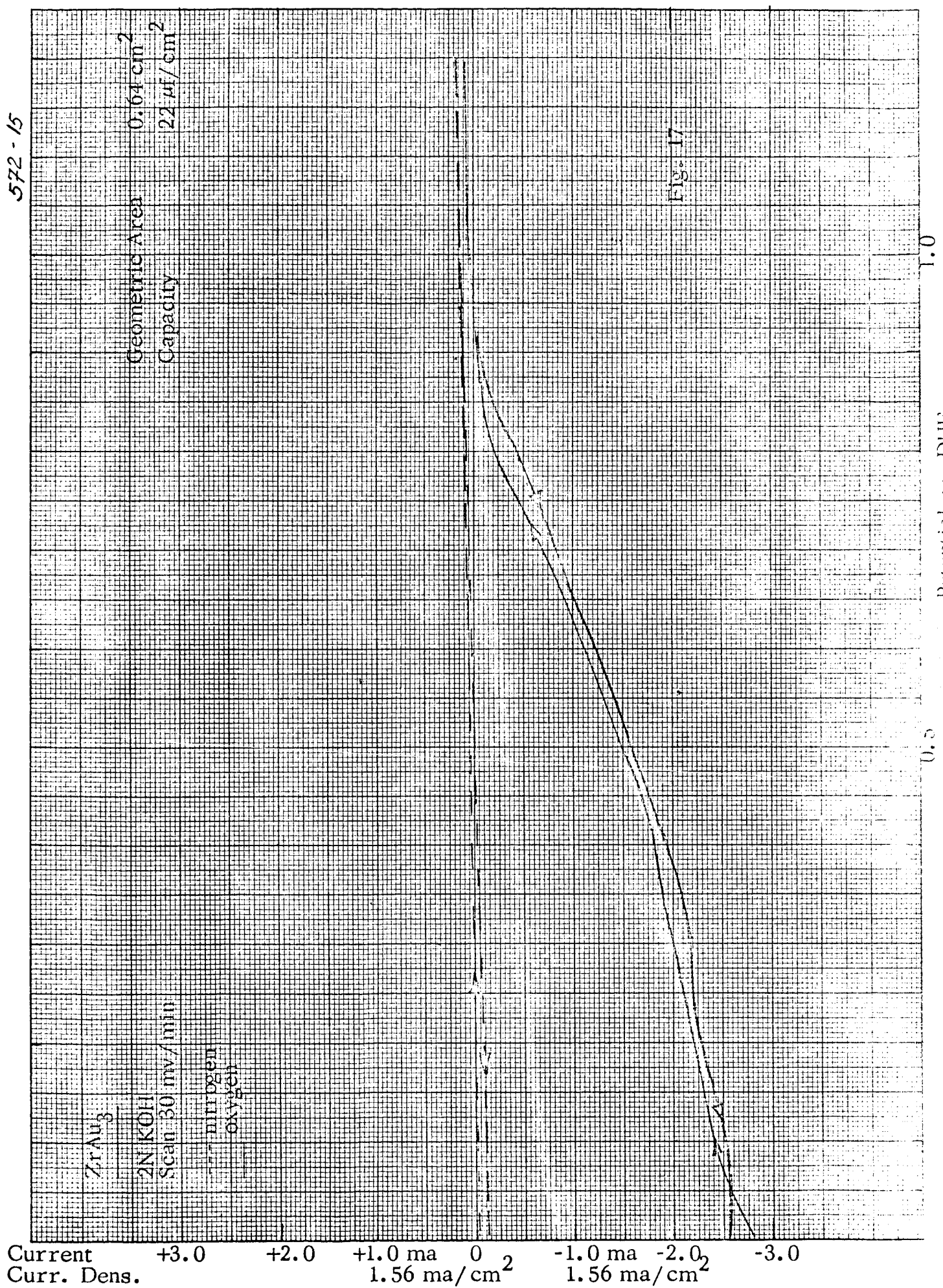
572-29



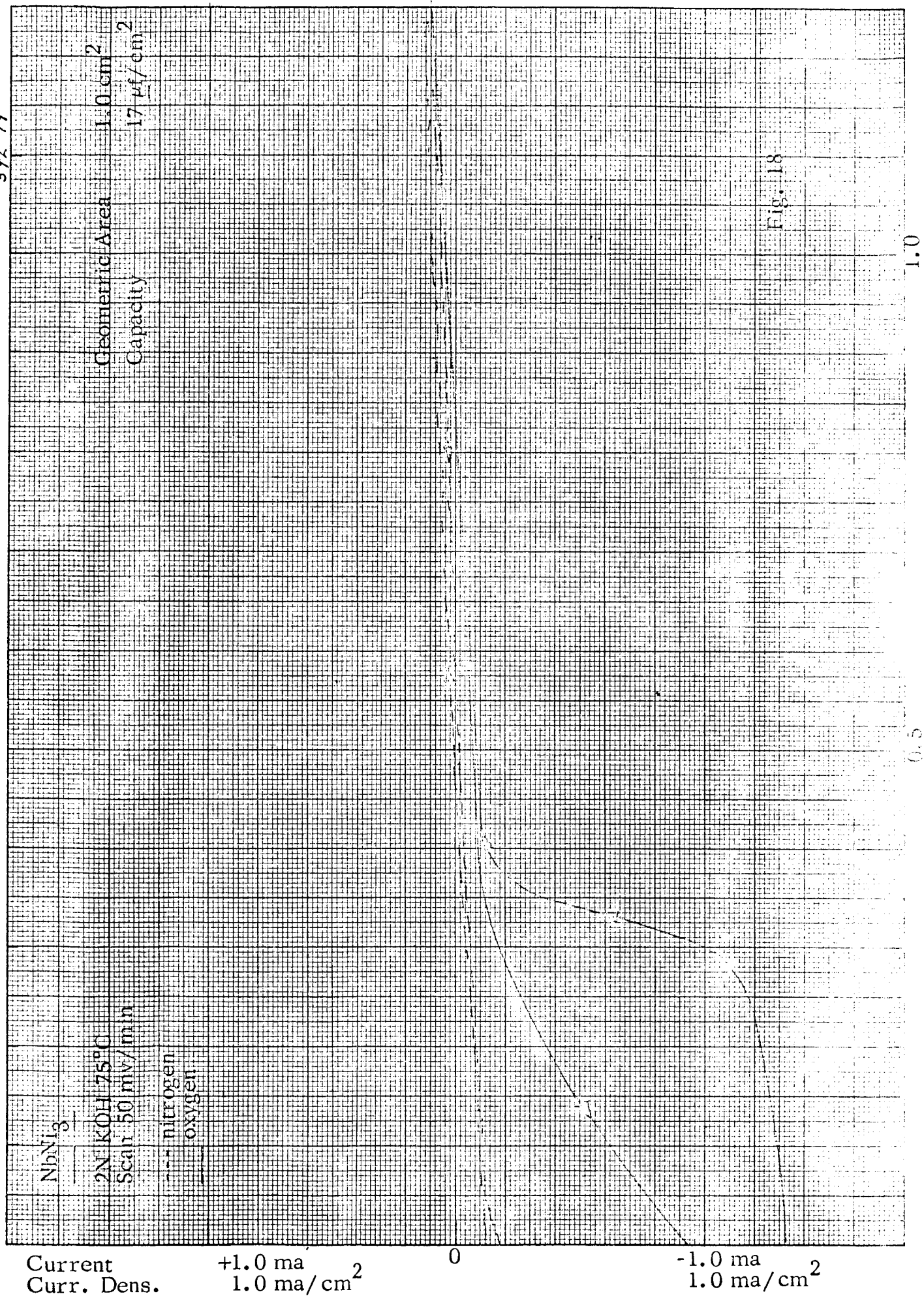
572-20



572-15



592-17



572-21

Geometric Area 0.86 cm^2
Capacity $21 \mu\text{f}/\text{cm}^2$

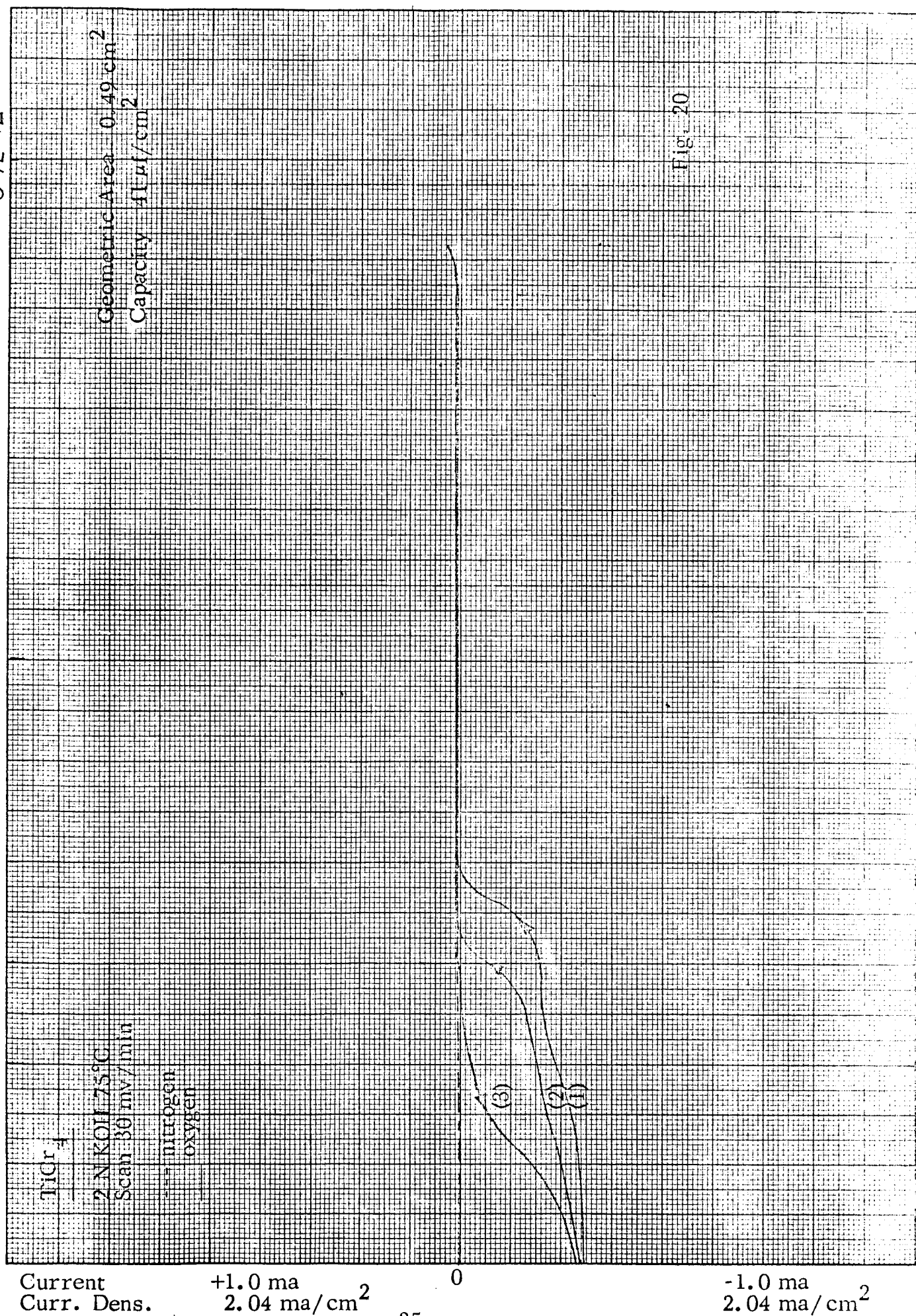
TiNi_3
2N KOH 75°C
Scan 50 mv/min
--- nitrogen
--- oxygen

Current
Curr. Dens. $+1.0 \text{ ma}$ $1.16 \text{ ma}/\text{cm}^2$ 0 -1.0 ma $1.16 \text{ ma}/\text{cm}^2$

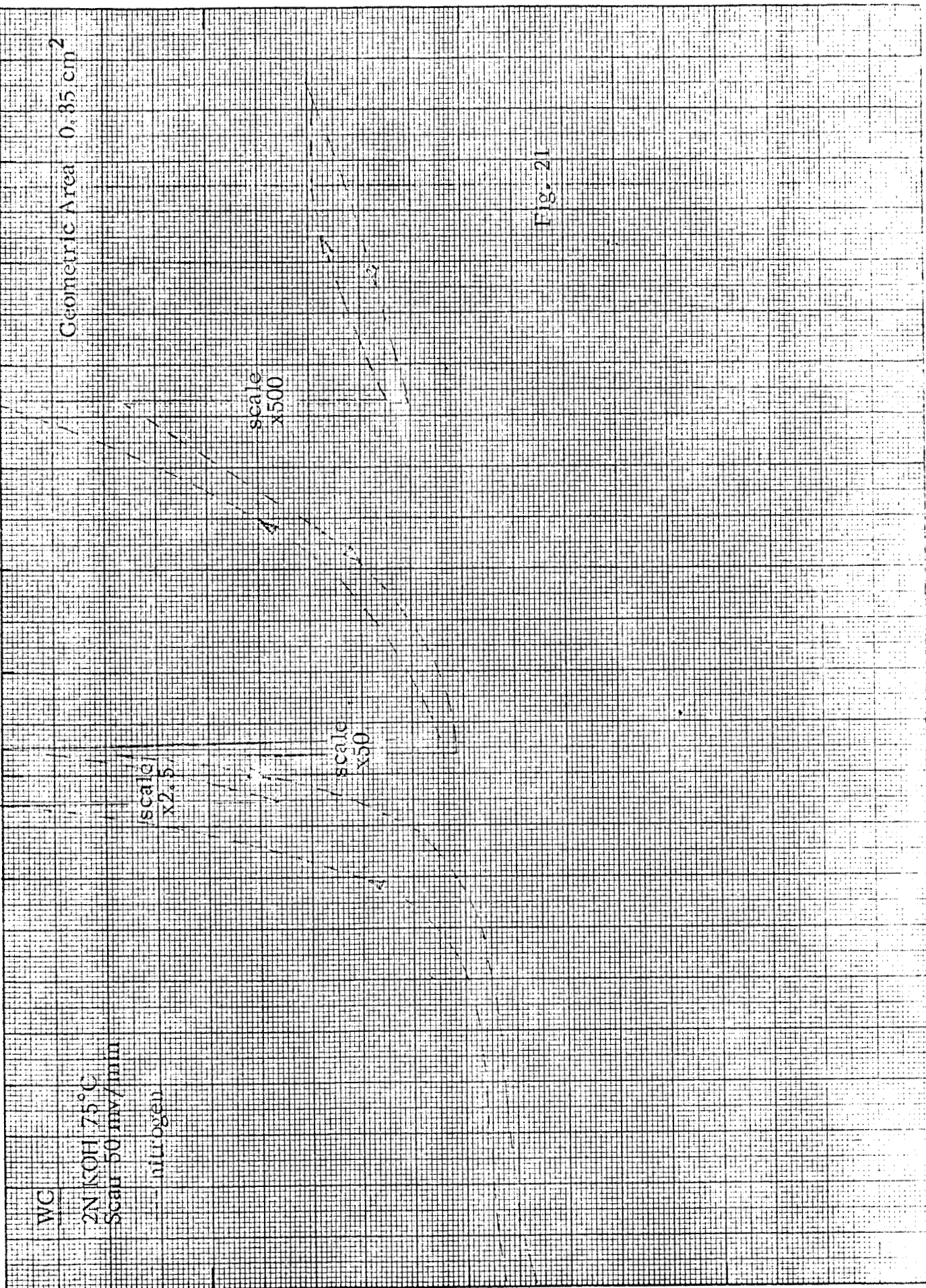
scale
 $\times 10$

Fig. 19

572-12



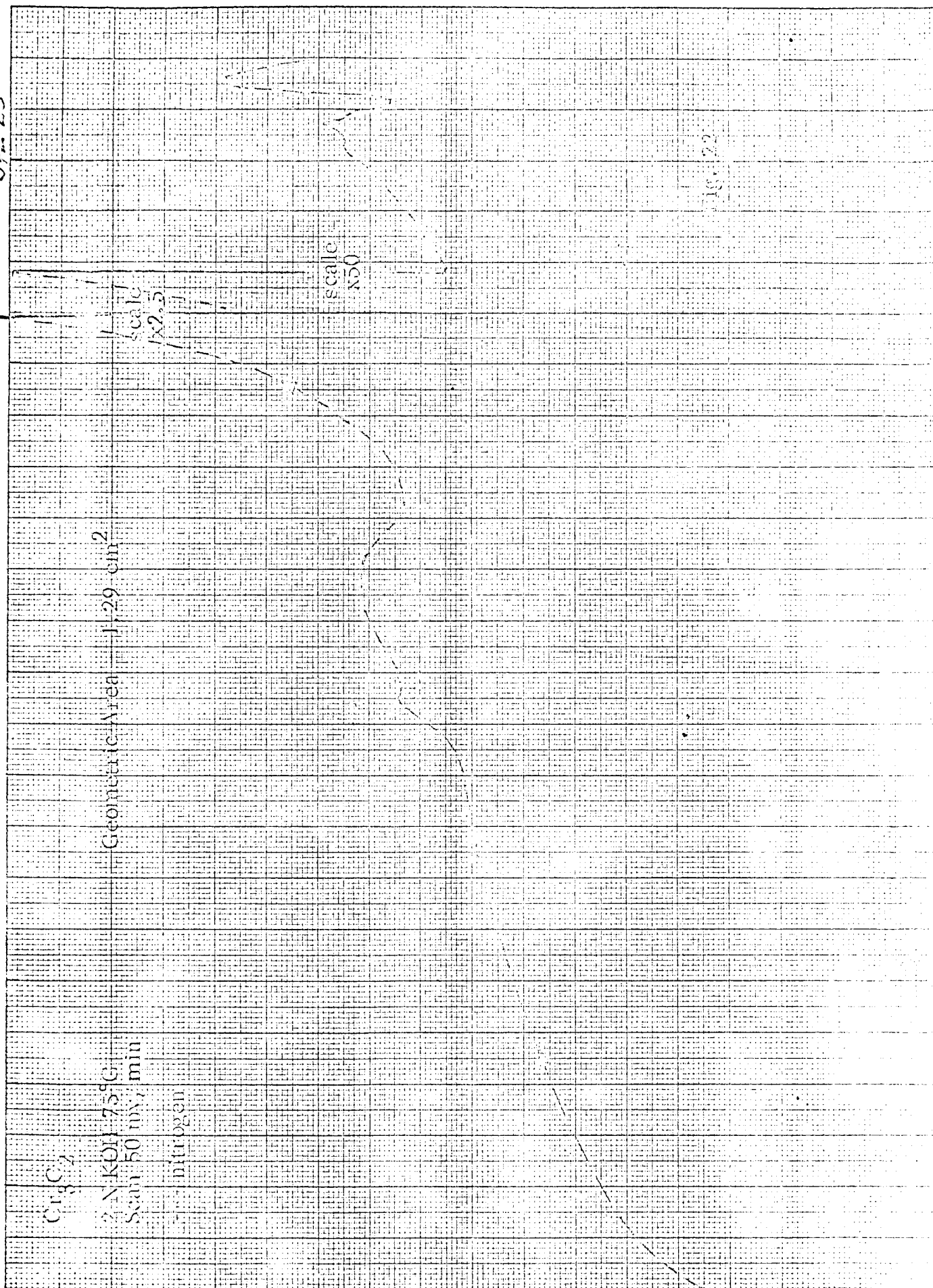
572-26



Current Curr. Dens. +1.0 ma 2.9 ma/cm² 0 -1.0 ma 2.9 ma/cm²

Potential vs. DHE 0.5 1.0

542-23



Current Density: $+1.0 \text{ ma}$ 1.55 ma/cm^2 0 -1.0 ma 1.55 ma/cm^2
 Curr. Dens.

572-24

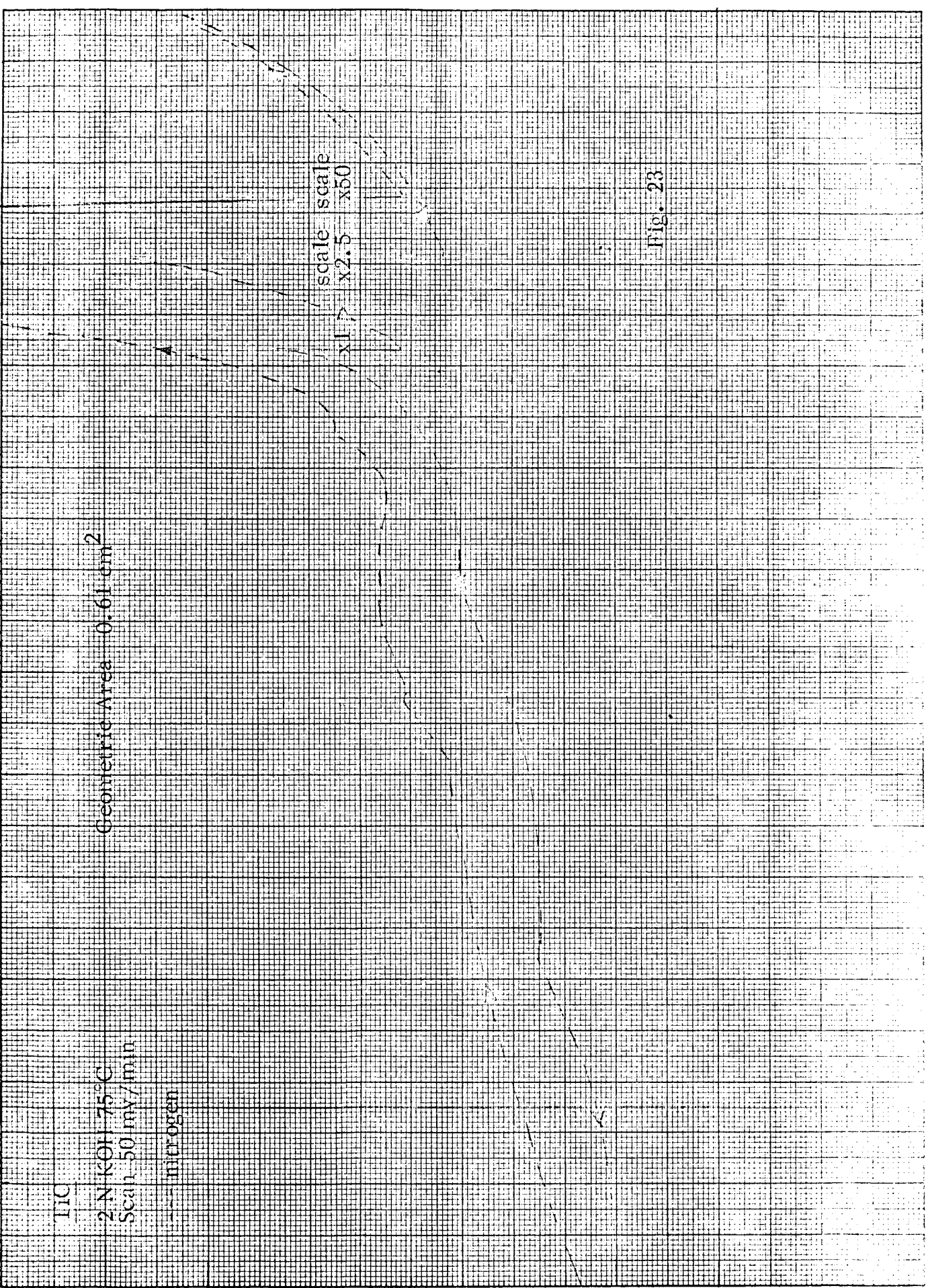
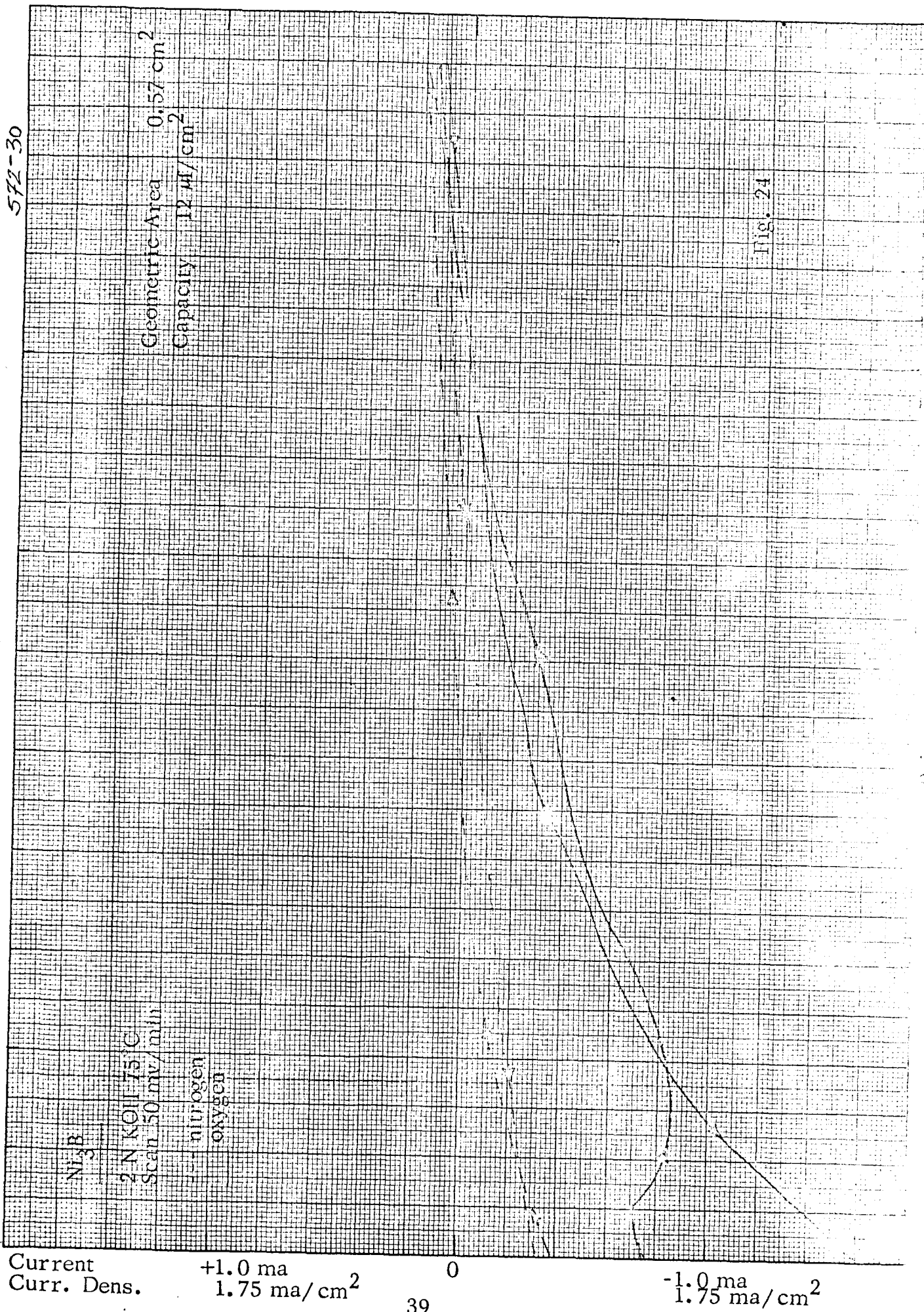


Fig. 23

Current
 Curr. Dens. +1.0 ma 1.64 ma/cm² 0 -1.0 ma 1.64 ma/cm²

572-30



experiments, as explained above. In addition, it can be seen that under similar conditions (2 N KOH and 75°C) gold has activity similar to platinum (compare current at 900 mv). The shape of the curve obtained in the direction of cathodic potentials (especially the indication of two steps) may mean that after anodic prepolarization the second step of the O_2 -reduction, $H_2O_2 \rightarrow H_2O$, is inhibited to a greater extent than after cathodic polarization (gold may be more sensitive than platinum to poisoning in this region).

Silver (Fig. 6): Silver shows, at 0.8 volts polarization, a very sizeable O_2 -reduction current. This agrees with results obtained elsewhere by several groups with porous electrodes. There are also clear indications of oxidation of the metal at higher potentials. This oxidation causes the activity of the electrode to decrease as shown by the hysteresis loop in the activation controlled region.

Tantalum (Fig. 7): Corrosion is low; activity for O_2 -reduction is also very low.

B. Intermetallic Compounds

At this stage of the program, the materials tested are scattered without logical order through the classification of Appendix A. Even with these materials not all the tests have been yet performed (for instance, data on metallographic analysis are incomplete); this characterization will be completed in the immediate future. It is expected that as more materials are investigated, filling the holes in the systematic classification of Appendix A, comparison of the various compounds will show general trends with respect to the importance of structure vs. atomic composition. At that point, materials will be selected to confirm or extend the findings. Special emphasis will be placed on interstitial and substitutional compounds (borides, carbides, nitrides, and oxides).

Some comments on the $i(E)$ -curves of the materials tested are given below, and finally, a summary table with values of current

density at several potentials is given (Table I). These values are of a relative and semiquantitative nature indicating trends rather than absolute figures.

A₂B - Stoichiometry

Zr₂Ni (CuAl₂-type, C16 structure) (Fig. 8):
corrosion is moderate; O₂-activity is low but not insignificant.

AB - Stoichiometry

TiNi (C₅Cl-type, B2 structure) (Fig. 9):
corrosion is excessive although passivation with time is possible; (large hysteresis). Activity for O₂-reduction is low but not insignificant.

NbPt (AuCd-type, B19 structure) (Fig. 10):
corrosion is excessive, although decrease with time is possible.
Activity for O₂-reduction is high.

TiCu (CuAu-type, L1₀ structure) (Fig. 11):
high corrosion current showing little decrease with time. Activity for O₂-reduction is very low at potentials higher than 500 mv.

AB₂-Stoichiometry

TaPt₂ (Fig. 12) (c.p. orthorhombic phase):
corrosion is very low; activity for O₂-reduction is equal or better than pure Pt. (It may be a way of diluting Pt).

AB₃ - Stoichiometry

TiPt₃ (AuCu₃-type, L1₂ structure) (Fig. 13):
Although only moderate corrosion is found in the N₂-i(E)-curve and in the O₂-i(E)-curve in the direction of decreasing potentials, the O₂-i(E)-curve obtained in the direction of increasing potentials shows very high anodic currents. This apparent contradiction has to be clarified.
Activity for O₂-reduction is good.

TaNi₃ (12 l s h - type, orthorhombic structure) (Fig. 14): corrosion is low. Activity for O₂-reduction is low at potentials lower than 400 mv.

TaPt₃ (12 l s h - type, DO_a structure) (Fig. 15): corrosion is high, with some small decrease with time. A strong anodic current is encountered in O₂-i(E)-curve taken in anodic direction, (similar to the one observed with TiPt₃). Activity for O₂-reduction is good.

It is interesting to observe that TaPt₃ corrodes considerably more than TaPt₂, in spite of the larger Pt concentration. This may be a structural effect.

TiCu₃ (2 l s h - type, orthorhombic structure) (Fig 16): corrosion is very high in the potential range of O₂-reduction; activity for O₂-reduction is very low at potentials higher than 500 mv.

ZrAu₃ (2 l s h - type, orthorhombic structure) (Fig. 17): corrosion is very low. Activity for O₂-reduction is high, although current does not increase abruptly with increasing polarization and no well defined limiting current exists.

NbNi₃ (TiCu₃-type, orthorhombic structure) (Fig. 18): corrosion is very moderate; activity for O₂-reduction is very low at potentials higher than 400 mv.

TiNi₃ (DO₂₄ structure) (Fig. 19): corrosion is high. There are two strong anodic peaks with two corresponding cathodic peaks which are not characteristic for Ni or for Ti. This point should be confirmed. The activity for O₂-reduction cannot be estimated due to the large corrosion current.

AB₄ Stoichiometry

TiCr₄ (A2 structure) (Solid solution at elevated temperature) (Fig. 20): corrosion is low at potentials below 1 volt. Activity for O₂-reduction is very low at potentials higher than E = 0.4 volt.

Interstitials

WC (B_h structure) (Fig. 21): corrosion is extremely high in potential range of O_2 -reduction; no sizeable decrease of current with time is apparent.

Cr₃C₂ ($D5_{10}$ structure) (Fig. 22): corrosion is extremely high in potential range of O_2 -reduction; no decrease of current observed when keeping potential constant at 900 mv.

TiC ($B1$ structure) (Fig. 23): corrosion is extremely high; no sizeable decrease of current with time is observed.

Ni₃B (DO_{11} structure) (Fig. 24): corrosion is moderately high at potentials of O_2 -reduction. Activity for oxygen reduction is moderate.

C. Corrosion Studies with Powders - Carbides

At the beginning of the program the only materials immediately available were various carbides in the form of -325 mesh powders and four alloys also in the form of -325 mesh powders. These materials were tested for corrosion by a manual potentiostatic method, i. e. the current was measured at controlled potentials from 0 to 1200 mv in a KOH solution saturated with N_2 . The electrodes were stationary and the runs were made in 35% KOH at 80°C. The powder electrodes were made by mixing the powder with Elvax trichloroethylene, applying to a nickel screen, and air-drying. This method has the disadvantages that the real surface is difficult to measure in the presence of a binder and that a current corresponding to corrosion can be measured only for particles in contact with both the electrolyte and the nickel screen. The results of these tests are given in Table II. In view of the dubious and qualitative nature of the data obtained from these powder electrode techniques, most of the above-mentioned materials will be re-run on the rotating disc electrode system as ingots or hot-pressed powders, and the powder electrode technique will not be used further for corrosion screening.

Table II
Powder Electrodes

		<u>N₂ - Corrosion Current ($\mu\text{a}/\text{cm}^2$)</u>	
	<u>Potential</u>	<u>1000 mv</u>	<u>800 mv</u>
ZrC	Increasing	+25	+20
	Decreasing	0	-5
TaC	Increasing	+1, 200, 000	+45, 000
	Decreasing	+1, 200, 000	+70, 000
Mo ₂ C	Increasing	+13, 000	+15, 000
	Decreasing	+4, 000	+3, 000
TiC	Increasing	+30	+55
	Decreasing	+5	0
Cr ₃ C ₂	Increasing	+115	+20
	Decreasing	+40	0
NbC	Increasing	+55	+60
	Decreasing	+15	+5
WC	Increasing	+175	+195
	Decreasing	+60	+150
HfC	Increasing	+75	+120
	Decreasing	+60	+20
Nb Re ₃	Increasing	+11, 000	+7, 000
	Decreasing	+4, 500	+4, 000
Ta ₃ Ir	Increasing	+700	+600
	Decreasing	+525	+425
W ₂ Hf	Increasing	+50	+50
	Decreasing	+50	+40

APPENDIX A
CLASSIFICATION OF COMPOUNDS BY STRUCTURE

We will consider initially alloys and compounds of the type



where T is a transition element and B a nontransition element belonging to groups IIA through VIA. In the T - B class we will consider especially beryllides, borides, carbides, silicides, antimonides, nitrides, phosphides, and oxides. Later on, we will include ternary systems, e.g. boronitrides, nitrocarbides, etc.

1) T - T: Alloys and compounds of the type A_xB_y are considered (note: both A and B are transition elements, A being to the left of B. We follow here the classical terminology at the risk of confusion between this B and the B elements above).

<u>Stoichiometry</u>	<u>Structure</u>	<u>Typical Members to be Examined</u>
A_3B	"β. W"	Ti_3Au
		V_3Ir
		Cr_3Pt
		Nb_3Pt
		Mo_3Pt
A_2B	$CuAl_2$ -type	Zr_2Ni
		Ta_2Ni
	$MoSi_2$ -type	Zr_2Pd
		Zr_2Au
		Ti_2Cu

<u>Stroichiometry</u>	<u>Structure</u>	<u>Typical Members to be Examined</u>
AB	Ti ₂ Ni-type	Ti ₂ Ni Hf ₂ Ir Hf ₂ Pt
	CsCl -type	TiCo TiNi TiRu
		NbPt
		TaRu
	β-VIr-type	VIr
		TaV ₂
		HfW ₂
		TiCr ₂
	Laves Phases	ZrIr ₂
		NbNi ₂
AB ₂	MoSi ₂ -type	ZrPd ₂
		TaNi ₂
		NbPt ₂
		TaPt ₂
	c. p. -phases	TiPt ₃
		ZrIr ₃
		CoPt ₃
		ZrPt ₃
	AuCu ₃ -type	
AB ₃		

<u>Stoichiometry</u>	<u>Structure</u>	<u>Typical Members to be Examined</u>
AB _n , n > 3	12 l sh	TaNi ₃
		TaPt ₃
		TaIr ₃ -TaPt ₃
	2 l sh	ZrAu ₃
		TiCu ₃
	3 l sh	VPt ₃
		MoNi ₄
		ZrAu ₄
		ZrNi ₅
		ThIr ₅
	Variable	Nb-Pt
		Ta-Ir
		Ta-Au
		Nb-Re
		Ta-Os
	χ	
	μ	TaNi
	σ	MoNi

2) T - B: Initially we will examine in the T - B series the following carbides and nitrides:

Carbides

Co₃C, Cr₃C₂, Mn₃C, Fe₃C

Co₂C, Cr₇C₃, V₂C, Mn₅C₂, Mo₂C, Nb₂C, Mn₇C₃

VC, ZrC, HfC, MoC, NbC, TaC, TiC, WC

TaC₂

Nitrides

Ag_3N , Ni_3N , $\gamma\text{-Co}_3\text{N}$, Mn_4N , Fe_4N

Fe_2N , $\gamma\text{-Mo}_2\text{N}$, $\delta\text{-Co}_2\text{N}$, $\epsilon\text{-Cr}_2\text{N}$, Mn_2N , Re_2N

CrN , HfN , ZrN , VN , TiN , $\epsilon\text{-TaN}$, NbN , $\delta\text{-MoN}$

Subsequently, ternary systems, including nitrocarbides will be examined.

APPENDIX B

DETERMINATION OF THE DOUBLE LAYER CAPACITY

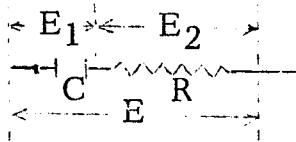
When the potential of an electrode is varied, a current flows equal to

$$i_c = C_D \frac{dE}{dt} \quad (C_D = \text{double layer capacity})$$

required to charge the double layer. Accordingly, if a triangular wave $\frac{dE}{dt} = \alpha \equiv \text{constant}$ of small peak-to-peak amplitude (≤ 100 mv) is applied to a working electrode which behaves as a pure condenser (i. e. without faradaic current or ohmic resistance), a current square-wave results. The peak-to-peak amplitude of this square wave is equal to $i_c = 2 \alpha C_D$, i. e. proportional to the double layer capacity and therefore to the real surface. A convenient way of using this method is to apply the triangular wave, superimposed on a dc-voltage (selected to avoid faradaic current) to the reference input of a potentiostat. The resulting current wave can be recorded by using the y-input of an x-y oscilloscope for the current wave and the x-input for the triangular voltage wave. The resulting oscilloscopic trace is, in the case of a perfect condenser, a rectangular current-voltage box. This method is subject to similar limitations as the ac methods. Its main advantage is that from the form of the $i(t)$ curve (or $i(E)$ box) the validity of the assumption that the electrode behaves as a pure condenser can be verified and conditions to reduce the deviations from this assumption can be more easily found than when working with sinusoidal ac. In the following examples, conditions have been selected in which the effect of faradaic currents and ohmic resistances can be easily calculated and corrected.

Case 1: Ohmic resistance in series with the condenser -

$$E = E_1 + E_2 \quad (1)$$



$$C \frac{dE_1}{dt} = i \quad (2)$$

$$\frac{dE}{dt} = \alpha \quad (3)$$

$$iR = E_2 \quad (4)$$

Differentiating Eq. (1) and substituting in the resulting differential equation one obtains:

$$\frac{di}{dt} + \frac{i}{RC} - \frac{\alpha}{C} = 0 \quad (5)$$

This linear differential equation can be easily integrated to give:

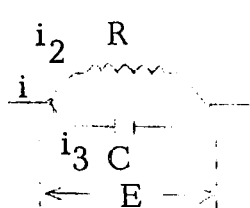
$$i = C\alpha + k \exp - \frac{t}{RC} \quad (6)$$

In the case of a single linear pulse at $t = 0$, $i = 0$ and

$$i = C\alpha (1 - \exp - \frac{t}{RC}) \quad (7)$$

The current will change as a function of time (voltage) and become equal to the capacity current when $\exp - \frac{t}{RC} \ll 1$. Obviously by keeping RC small the time necessary to measure the pure capacity current will become smaller.

Case 2: Ohmic resistance in parallel to the condenser



$$i = i_1 + i_2 \quad (8)$$

$$i_1 = C \frac{dE}{dt} \quad (9)$$

$$\frac{dE}{dt} = \alpha \quad (10)$$

$$i_2 = \frac{E}{R} \quad (11)$$

Substituting in Eq. (8) gives:

$$i_i = C \alpha + \frac{E}{R} \quad (12)$$

(for the increasing potential sweep)

or

$$i_d = -C \alpha + \frac{E}{R} \quad (13)$$

(for the decreasing potential sweep)

or

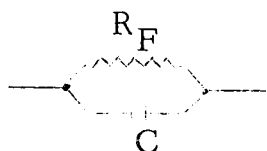
$$\Delta i = i_i - i_d = 2C\alpha \quad (14)$$

This case is unusual in electrochemistry.

Case 3: Activation controlled faradaic current coupled to the capacity.

This case is a variation of case 2, and may frequently occur in electrochemical systems.

Similarly to case 2, one obtains:



$$i_i = C \alpha + i_0 \exp \frac{\alpha n F E}{R T} \quad (15)$$

(for the increasing potential sweep) and

$$i_d = C \alpha + i_0 \exp \frac{\alpha n F E}{R T} \quad (16)$$

(for the decreasing potential sweep)

or

$$\Delta i = 2 C \alpha \quad (17)$$

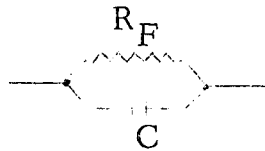
i. e. if the method is used under these conditions, from the difference between increasing and decreasing sweep, C_D can be found. By varying α these conditions can be confirmed.

If diffusion polarization is present, the resulting diffusion impedance is a combination of capacity and resistance which changes with time. Although the problem can be solved by integration of Fick's second law, its solution is outside the scope of this presentation. Only in the region of the limiting current is the determination of C_D possible without using involved calculations, as shown in the following:

Case 4: Capacity measurement in the region of a diffusion limiting current (i_L). This very special case is similar to cases 2 and 3.

$$i_i = C \alpha + i_L \quad (18)$$

Similarly to case 2, one obtains:



$$i_i = C \alpha + i_0 \exp \frac{\alpha n F E}{R T} \quad (15)$$

(for the increasing potential sweep) and

$$i_d = C \alpha + i_0 \exp \frac{\alpha n F E}{R T} \quad (16)$$

(for the decreasing potential sweep)

or

$$\Delta i = 2 C \alpha \quad (17)$$

i. e. if the method is used under these conditions, from the difference between increasing and decreasing sweep, C_D can be found. By varying α these conditions can be confirmed.

If diffusion polarization is present, the resulting diffusion impedance is a combination of capacity and resistance which changes with time. Although the problem can be solved by integration of Fick's second law, its solution is outside the scope of this presentation. Only in the region of the limiting current is the determination of C_D possible without using involved calculations, as shown in the following:

Case 4: Capacity measurement in the region of a diffusion limiting current (i_L). This very special case is similar to cases 2 and 3.

$$i_i = C \alpha + i_L \quad (18)$$

and

$$i_d = -C \alpha + i_L$$

or

$$\Delta i = i_i - i_d = 2 C \alpha .$$

In addition to these simple cases, there are many combinations of faradaic and ohmic resistances. Therefore, measurements will be made preferably in the absence of faradaic current, minimizing ohmic resistances. When faradaic currents are unavoidable, regions of pure activation control or of diffusion limiting current will be selected.